Cerebral Cortex, May 2020;30: 2834–2853

doi: 10.1093/cercor/bhz278
Advance Access Publication Date: 16 December 2019
Original Article

ORIGINAL ARTICLE

Brain Morphological Dynamics of Procrastination: The Crucial Role of the Self-Control, Emotional, and Episodic Prospection Network

Zhiyi Chen[1,2], Peiwei Liu[3], Chenyan Zhang[4] and Tingyong Feng[1,2,*]

[1]Faculty of Psychology, Southwest University, Chongqing, China, [2]Key Laboratory of Cognition and Personality, Ministry of Education, Chongqing, China, [3]Department of Psychology, University of Florida, Gainesville, USA, and [4]Cognitive Psychology Unit, The Institute of Psychology, Faculty of Social and Behavioural Sciences, Leiden University, Gainesville, Netherlands

Address correspondence to Tingyong Feng, School of Psychology, Southwest University, No. 2, Tian Sheng RD, Beibei, Chongqing 400715, China. Email: fengty0@swu.edu.cn

Abstract

Globally, about 17% individuals are suffering from the maladaptive procrastination until now, which impacts individual's financial status, mental health, and even public policy. However, the comprehensive understanding of neuroanatomical understructure of procrastination still remains gap. 688 participants including 3 independent samples were recruited for this study. Brain morphological dynamics referred to the idiosyncrasies of both brain size and brain shape. Multilinear regression analysis was utilized to delineate brain morphological dynamics of procrastination in Sample 1. In the Sample 2, cross-validation was yielded. Finally, prediction models of machine learning were conducted in Sample 3. Procrastination had a significantly positive correlation with the gray matter volume (GMV) in the left insula, anterior cingulate gyrus **(ACC), and parahippocampal gyrus (PHC) but was negatively correlated with GMV of** dorsolateral prefrontal cortex (dlPFC) **and gray matter density of ACC. Furthermore, procrastination was positively correlated to the cortical thickness and cortical complexity of bilateral** orbital frontal cortex **(OFC). In Sample 2, all the results were cross-validated highly. Predication analysis demonstrated that these brain morphological dynamic can predict procrastination with high accuracy. This study ascertained the brain morphological dynamics involving in self-control, emotion, and episodic prospection brain network for procrastination, which advanced promising aspects of the biomarkers for it.**

Key words: brain morphology, large-scale networks, procrastination, surface-based morphometry, voxel-based morphometry

Introduction

Procrastination was considered to parallel the evolution of the human civilization throughout whole historical span (Knaus 2000; Gustavson et al. 2015). The advents of the industrial revolution and the information era promoted the societies technically. The accompanied commitments and deadlines could result in procrastination straightforward. As refined by Steel (2007), procrastination refers to the predisposition for voluntarily putting off the scheduled courses of action even though this would lead to a worse outcome in the daily life around the world (Steel 2007). Behavioral procrastination is predominantly ubiquitous to us: the chronic procrastination is afflicting about 15–20% adults (Harriott et al. 1996); 70–80% of undergraduates report the premonitory symptoms of procrastination, and 20%

of population do fall victim to procrastination in the academic achievements and social communication (Esteban and Ramírez 2014). In this vein, the procrastination admits to substantial maladies linking to awful consequences, such as the poor subjective well-beings (Steel 2007; Steel and Klingsieck 2016), deficient fitness (Sirois 2004; Steel and Ferrari 2013), volatile financial status (Ferrari et al. 1995; O'Donoghue and Rabin 1999), and even devastating public policies (Lynch and Zauberman 2006).

Procrastination, as a complicated behavior, has been considered to be implicated in multiple processes, particularly in self-control, emotional repair, and future thoughts. Specifically, self-control was broadly argued as the mainstream for the account of the procrastination and further sparked intense interests in this domain (Van Eerde 2000; Ariely and Wertenbroch 2002; Steel 2010). Self-control is defined as a capacity that overriding dominant response tendencies for goals-unrelated stimuli and taking goal-congruent actions to support the pursuit of important goals (Bauer and Baumeister 2004; Bin et al. 2007). A substantial amount of studies provided evidence compelling that the individuals of higher self-control can outperform in pursuit of long-term utility, thus giving rise to lower procrastination remarkably (Ziesat et al. 1978; Ariely and Wertenbroch 2002; Digdon and Howell 2008). Emerged quantitative meta-analyses provided the more robust evidences: the procrastination can be attributed to the failure of the self-regulation to a large extent (Steel 2007; De Ridder and Lensvelt-Mulders 2018). Notably, this term was predefined as "how individuals exert self-control over their own responses in order to pursue long-term beneficial goals" (Baumeister and Vohs 2004). In other words, self-regulation served to a more general and superordinate concept than self-control, which might largely depend on the mechanism involving in self-control (McCullough and Willoughby 2009). Recently, emerging theoretical account has putted forward this idea compelling that the procrastination is due to the failure of self-regulation (Steel 2007, 2010). Further, an insightful scheme for the failure of the emotion regulation has been highlighted as well, which consistently accounts the procrastination as the sacrifice of long-term profits for the repair of the injured mood in tasks (Tice and Bratslavsky 2000; Tice et al. 2001; Sirois and Pychyl 2013; Sirois 2014a, 2014b). In other words, to mend the emotional harms from the engagement of task, the procrastinating behaviors would emerge when individuals experience the negative emotions toward task engagement (task aversiveness) more prior than the incentive delivery of task (outcome utility) (Zhang et al. 2019a, 2019b). Additionally, procrastination referred to decisions toward the future, and thus, the crucial role of episodic future thinking on the procrastination should be underscored. Generally, episodic future thinking referred to an ability to project oneself into the future for pre-experiencing an event (Atance and O'Neill 2005). The function of such faculty can be implicated in the far-sighted decisions, planning, and action (Boyer 2008; D'Argembeau et al. 2011; Schacter et al. 2012). Individuals who were triggered with episodic future thinking are more likely to prefer for long-term future outcome, thus promoting more far-sighted decisions (Peters and Büchel 2010; Benoit et al. 2011; Liu et al. 2013; Rebetez et al. 2016). In this vein, several lines of straightforward evidence implied that the high performance of episodic future thinking might bias evaluation on task for more long-term utility so that mitigating procrastination (Sirois and Pychyl 2013; Rebetez et al. 2016). On balance, emerging evidence was indicative of the potentials for neural substrates of procrastination in these interactive entities—namely self-control process, emotional regulation process, and episodic prospection process.

Thus far, the concerns for the neurobiological substrate of procrastination have been explored from a few tentative studies. Liu (2017) revealed that the local gray matter volume (GMV) losses in the left dorsolateral prefrontal cortex (dlPFC) for procrastinators for the first time (Liu and Feng 2017). Afterwards, Hu (2018) undertook the whole-brain analysis to ascertain brain structural pattern of procrastination with special regards to GMV in a large sample, demonstrating the intimate link between the GMV of parahippocampal gyrus (PHC), orbital frontal cortex (OFC), ventromedial prefrontal cortex (vmPFC), dlPFC, and procrastination (Hu et al. 2018). Meanwhile, outcomes which pertain to these brain structural characteristics of procrastination were undergirt by the emerging evidence (Liu and Feng 2018). Likewise, several resting-state functional magnetic resonance imaging (fMRI) studies further advanced some useful attempts to construe the in-depth neuronal pattern of procrastination as well. In terms of brain functional scheme, researches have unraveled the enhanced amplitude of low-frequency fluctuation of resting-state activation in the cluster of PHC and vmPFC for steep procrastination but observed the inhibiting local activity in anterior prefrontal cortex (Zhang et al. 2016). Recently, a task-related fMRI study indicated that procrastinator was more prone to delay tasks due to the disrupted PHC-striatal circuit (Zhang et al. 2019a). Aside from the identification for the local brain pattern, emerging studies also illuminated the predictive role of the dysfunctional connectivity within default mode network on the procrastinator (Wu et al. 2016; Zhang et al. 2016). From what has been reviewed briefly, it could be observed that despite the proliferation in the explorations for the neurobiological substrate of procrastination, the understanding for the brain structural pattern of procrastination is still constrained into the local GMV. An increasing need for expanding the understanding for the comprehensive brain morphological dynamics is emerging.

Owing to the technological revolutions, in addition to the canonical voxel-based morphometry (VBM) analysis for the sensitive quantification, the deformation-based morphometry (DBM) provided a striking tool for the sake of the robust detection on the brain morphometric dynamics as well (Ashburner and Friston 2000; Gaser et al. 2001). As an alternative method for the volumetric measure, DBM strove to capture the subtle differences between the spatially normalized brain space and the original one leveraging the nonlinear spatial registration (Gaser et al. 1999). Such differences for the local volume changes could be mathematically described as the Jacobian determinant, which was well known as a robust tensor for the estimation of alternations of each voxel (Chung et al. 2001; Gaser et al. 2001). DBM analysis has been widely adopted in the field of the classification for the patient cohorts and abnormal development of human brain, which shows acceptable validity and consistency in a considerable amount of researches (Cardenas et al. 2007; Yang et al. 2014; Kundu et al. 2018).

Notwithstanding this, it was evident that the measure for the volume of brain could just observe a little portion of multiple aspects of fruitful brain anatomical markers. There were increasing appeals for the objective characterization on neuroanatomical morphology with the shape of brain, such as cortical thickness (CT), gyrification, and surface complexity (Gerig et al. 2001; Escorial et al. 2015; Román et al. 2015; Maingault et al. 2016). CT is reported as an independent quantitative feature for the description of brain local changes between the pial surface and white surface, and it seems to be advantageous over volume

measures for exploration on the brain anatomy and even gene (Han et al. 2006; Sowell et al. 2007; Panizzon et al. 2009; Anderson et al. 2010). Besides, the gyrification of cortical surface is also considered as a novel approach to make use of the absolute mean curvature for the razor-sharp delineation into the cortical folding of brain (Luders et al. 2006). Aside from above measures, the common strategies used to investigate the brain morphological features are to gauge the cortical 3D complexity. Based on the spherical harmonic (SPH), local cortical complexity of brain surface is reconstructed with the von Koch fractal surfaces and further quantified as the fractal dimension (FD), with higher FD values for more complex local surface (Yotter et al. 2011b). Owing to the superior mathematical properties for the quantify of chaotic entities (i.e., human brain), it is of valuable to integrate cortical gyrification and 3D complexity for examining cortical folding of brain shape (Mangin et al. 2004; Fischl et al. 2007). In brief, the advent of novel approaches to characterize the brain structure provided more comprehensive evidence for the understandings of procrastination.

To fill this gap, this study takes advantage of above measures to propose a comprehensive understanding of the neural substrate of the procrastination from brain morphological dynamics. To achieve this purpose, the investigations for the brain morphological dynamics would be examined from the behavioral brain scheme and test-retested in the brain-behavioral reconfiguration. In detail, multiple linear model is designed to fit the procrastination to GMV, grey matter density (GMD), CT, gyrification, and surface 3D complexity of whole-brain voxels in the sample 1 ($n = 242$) respectively. To further substantiate the role of these brain structural alternations on procrastination, values were extracted from these brain regional masks derived from these findings in Sample 1 to cross-validate the reliability and reproducibility of the current study in the independent Sample 2. Afterwards, the step-wise multiple regression model leveraging the estimation of ordinary least square (OLS) method was conducted for the regression of these brain structural features against procrastination. Furthermore, L1 norm Least absolute shrinkage and selection operator (L1-LASSO) regression was undertaken as the reliability analysis to further verify above findings due to the intrinsic shortcomings of conventional OLS model. To overcome the growing concerns on the null hypothesis significant test (NHST), the Bayesian estimation model was implemented to acknowledge these findings. Ultimately, it is of also interest to know whether these brain structural dynamics can practically predict procrastination. In this vein, the support vector regression (SVR) algorithm embodied in machine leaning model was adopted for the further prediction of the procrastination.

As the increasing calls from the American Psychological Association and previous studies for pre-registration, the aims and hypotheses of the current study have been submitted at the Open Science Framework (OSF, website: https://osf.io/kdtp2/registrations) for the pre-registration (Kai and Cesario 2015; van't Veer and Giner-Sorolla 2016):

Aims

(1) The major aim is to utilize novel and advanced brain imaging techniques—namely DBM, CT, and cortical folding (i.e., gyrification and 3D complexity)—for obtaining the comprehensive understanding of brain morphological dynamics of procrastination.
(2) This study also strives to build a theoretical model based on brain network to account procrastination.

Hypotheses

(1) The neuroanatomical substrates of procrastination were not only observed for the dynamics of GMV in dlPFC, parahippocampus (PHC), insula, etc. but also extended for the variation of CT in these brain regions and the features of brain folding in these clusters;
(2) These brain morphological dynamics can be encapsulated into triple brain networks (systems): top-down self-control network (e.g., dlPFC, anterior cingulate gyrus [ACC], posterior cingulate cortex (PCC)), emotional regulation network (e.g., Insular, OFC), and even episodic future thinking network (e.g., PHC, Amygdala).

Materials and Methods

Participants

A total of 688 participants were recruited for the study composing of three independent samples (Sample 1: mean age 21.03, SD, 2.05, range 17–26, 112 males; Sample 2: mean age 20.87, SD, 2.03, range 17–26, 103 males; Sample 3: mean age 20.96, SD, 2.04, range 16–27, 103 males). Given the potential distortions of neuroimage the undue head motions (the degree of absolutely translation and rotation exceeds 2 mm) resulted in, six participants were removed from this study. Afterwards, three participants were also ruled out because these images were ranked as the E (critical) or F (unacceptable) from the automatic quality estimation (see below for details). Then, we drew on an evaluation for the sample size to guarantee the enough statistical power by using G*Power package (http://www.softpedia.com/get/Science-CAD/G-Power; (Faul et al. 2009). The result showed the satisfactory effect size (minimum sample size was required for 153 participants) for this study (Multilinear regression model, H1 $\rho^2 = 0.15$, type I error $\alpha = 0.05$, Power $1 - \beta = 0.95$; see Supplemental information [SI] Method).

Encouragingly, the sample size in this study can preserve the robustness of prediction performance in the machine learning as well, irrespective of which regression algorithm was conducted (e.g., OLS, LASSO, or Ridge Regression; (Lee et al. 2010; Trawiński et al. 2012). All participants were confirmed without the history of psychiatric or neurological illness by the canonical psychiatric clinical assessment; they were healthy adults with right-handed and normal or corrected-to-normal vision. No significant differences of each demographic information between genders/samples were identified (see Table 1). The protocol of this study has been formally approved from the Institutional Review Board (IRB) of the Southwest University (China).

Behavioral Measures

We adopted the 12-item pure procrastination scale (PPS) recently revised by Svartdal et al. (2017) to characterize the prevalence of behavioral procrastination (Svartdal and Steel 2017). A robust body of studies has widely leveraged this scale for the measure of one's procrastination in their studies, indicating the satisfactory psychometric properties and robustness (Svartdal 2017; Zhang et al. 2017; Rebetez et al. 2018). Typically, items of PPS described a routine scenario to evaluate the resemblance on a 5-point Likert-type scale from 1 (very uncharacteristic) to 5 (very characteristic); individuals with high total scores in this scale were generally prone to procrastination.

Comparatively speaking, PPS was the superior measure for the core properties of procrastination than alternative relevant scales (Svartdal and Steel 2017). What's more, the high internal

Table 1 Detailed demographic information for these participants

	Sample 1 ($n = 243$)		P_1	Sample 2 ($n = 215$)		P_2	Sample 3 ($n = 221$)		P_3	$P_{F\text{-test}}$
	Male	Female		Male	Female		Male	Female		
Numbers	112	131	–	103	112	–	65	156	–	–
Age	21.20 (2.1)	20.89 (2.0)	0.27	20.96 (2.1)	20.78 (1.9)	0.53	21.32 (2.1)	20.81 (1.9)	0.08	0.68
Education	13.20 (2.0)	12.89 (2.3)	0.23	12.96 (2.1)	12.78 (2.0)	0.52	13.32 (2.1)	12.81 (2.0)	0.07	0.69
Body Mass Index (BMI)	20.80 (2.7)	20.41 (2.4)	0.25	21.04 (2.9)	20.35 (2.5)	0.06	20.85 (2.4)	20.58 (2.8)	0.49	0.92
PPS score	34.83 (7.4)	33.52 (8.1)	0.19	34.93 (7.2)	33.61 (9.2)	0.24	34.26 (6.8)	34.31 (8.7)	0.96	0.96
Personality										
Conscientiousness	38.69 (4.1)	39.22 (3.9)	0.31	38.62 (4.0)	38.70 (4.1)	0.88	38.75 (4.1)	38.85 (4.1)	0.86	0.63
Extraversion	39.02 (4.2)	39.13 (4.2)	0.83	38.40 (4.5)	38.56 (4.4)	0.80	38.12 (4.5)	39.01 (4.2)	0.16	0.95
Neuroticism	36.79 (4.4)	36.13 (4.0)	0.58	37.03 (4.5)	36.94 (4.2)	0.87	36.35 (4.0)	36.92 (4.5)	0.37	0.75
Agreeableness	36.50 (4.1)	36.90 (3.6)	0.41	36.96 (4.4)	37.42 (3.9)	0.41	36.78 (3.8)	36.98 (3.9)	0.73	0.43
Openness	37.23 (4.2)	37.71 (4.1)	0.37	37.05 (4.6)	37.65 (4.6)	0.33	37.01 (4.4)	37.69 (4.5)	0.30	0.36

consistency reliability (Cronbach's $\alpha = 0.92$) and discriminant/-convergent validity (average variance extracted (AVE) > squared correlations (SC) > 0.05) were predominantly found in this scale, highlighting the robustness in the cross-cultural context as well (Rozental et al. 2014; Svartdal 2017; Svartdal and Steel 2017; Rozental et al. 2018). In addition, Neuroticism Extraversion Openness Personality Inventory (NEO-PI) was adopted as the robust tool to characterize the personality traits as the covariable of no interest in the model. This scale was widely considered reliable and practical in the cross-cultural contexts (Costa et al. 1991; Costa and McCrae 1992). Likewise, the subscale of the State-Trait Anxiety Inventory developed by Spielberger was applied to test the prevalence of trait anxiety, which was proven to be reliable for its statistical properties (Spielberger and Gorsuch 1983).

Structural MRI Protocol

All the acquisitions pertaining to the high-resolution anatomical images from three independent samples were undertaken from the same center (i.e., Key Laboratory of Cognition and Personality, Ministry of Education, China). These images were collected with the Siemens Trio MRI scanner of 3 Tesla (Siemens Medical Department, Erlangen, Germany). The 16-channal head coil of circular polarization was applied to the record of high-resolution T1-weighted images ($1 \times 1 \times 1.33$ mm^3), which is in conjunction with foam padding for the constraint of head motion. During scanning, the magnetization-prepared rapid gradient echo pulse sequence was utilized (128 slices of contiguous sagittal maps; time repetition = 2530 ms; time echo = 3.39 ms; flip angle = 7°; field of view; (FoV) = 256×256 mm^2).

Preprocessing and Analysis

Voxel-Based Morphometry

These anatomical images underwent the remarkable productive preprocessing via Computational Anatomy Toolbox (CAT12 r1318, http://dbm.neuro.uni-jena.de/cat/) toolbox implemented in the Statistical Parametric Mapping (SPM) 12 package (http://www.fil.ion.ucl.ac.uk/spm/software/spm12/). Even though CAT12 functions to segmentation of anatomical images in the SPM12, it deviates significantly from the native segmentation strategy and has been broadly proven a more potent and practice approach for brain morphological analysis relative to alternatives (Farokhian et al. 2017; Cigdem et al. 2018). Emerging evidence have indicated that the CAT12 can provide more robust and accurate results for volumetric estimations than the conventional VBM8 toolbox (Farokhian et al. 2017).

Specifically, CAT12 implemented in the SPM12 would call the returns from the self-definition diffeomorphic anatomical registration through exponential lie algebra (DARTEL) template and more fruitful built-in algorithms or protocol pertaining to brain segmentation (Gaser and Dahnke 2016). There were several powerful strengths for the CAT12: (1) it could provide more accurate brain images using internal interpolation in poor resolution images and anisotropic spatial resolutions, (2) CAT12 can perform well for the denoising of brain images since both spatial-adaptive non-local means (SANLM) and Markov random field were undertaken simultaneously (Rajapakse et al. 1997; Manjón et al. 2010), (3) CAT12 initiates the partial volume estimation (PVE) with a simplified mixed model of a maximum of two tissue types for segmentation, which can reap huge fruitful for the in-depth segmentation in mixed classes of gray matter (GM)-cerebrospinal fluid (CSF) (Gaser and Dahnke 2016). Thus, the main analyses of brain images were carried out using CAT12 in the current study.

All anatomical images were first spatially corrected by manually reoriented the alignment of anterior commissure-posterior commissure at the native space of Montreal Neurological Institute (MNI) in favor of better image registration (Talairach et al. 1988). Subsequently, the internal interpolation method was concatenated to reduce the routine strip artifacts when co-registering the native images to the MNI space with affine transformation of bias-field correction. In this stage, 12 parameters of affine registration leveraging mean square variants were estimated to generate the vectors of the basic function for the sake of the minimization of the residual error between the original images and predetermined template. Afterwards, the SANLM denoising filter for images of intensity normalization was applied to further dislodge noises stemming from the heterogeneity of cranial morphology (intensity inhomogeneities) within the head coil, whose default threshold depended on the automatic estimation for the residual noise in these images (Manjón et al. 2010). Furthermore, the adaptive maximum a posterior (AMAP) segmentation protocol was undertaken to subserve the segmentation from whole-brain tissue into GM, white matter (WM), and CSF without the requirement for the priori information derived from tissue probability maps (Gaser and Dahnke 2016).

Aside from AMAP process, a mixed model of a maximum of two tissue types was also constructed to conduct the partial volume evaluation (PVE) for more potent segmentation (Tohka et al. 2004). Prior to formal segmentation with AMAP protocol, the local adaptive transformation of intensities of all the brain tissues was implemented to preserve from the risk of underestimating the GM or overrating the CSF due to the anisotropic intracranial backgrounds (e.g., iron content of distinct cortices) (Cardoso et al. 2013). Subsequently, we combined the nonlinear spatial DARTEL strategy and Geodesic Shooting algorithm to jointly normalize these preprocessed images into MNI space (Ashburner 2007; Ashburner and Friston 2011). Here, the group template was produced from Information eXtraction from Images (IXI)-database (http://www.brain-development.org) consisting of 555 healthy control subjects and was available in the normalization of MNI space for the six different iteration steps. Ultimately, the CAT12 provided an automatic tool to drive the revised skull stripling based on the graph and the new "clean up" for the remnant brain tissues of no interests such as meninges and other volumes. The default parameter ($\varepsilon = 0.5$) of these processes was adopted for the moderate constraint, which has been broadly accepted in previous studies (Besteher et al. 2017; Ide et al. 2017). Taking the compensate of inexact information of spatial normalization and the need for the noise-signal ratio of neuroimages into account, all the modulated-normalized images were smoothed with a Gaussian kernel of 8 mm full width at half maxima (FWHM).

Deformation-Based Morphometry

For detecting the subtle local alterations between two spatially normalized brain images in the anatomical displacement fields, DBM was undertaken as well. Compared with the conventional volumetric approach based on the manual segmentation, DBM could reap more huge fruits from the superior local sensitivity and higher resolution of the deformation field-based maps using the nonlinear and nonrigid registration procedures for the adaptive brain template and adjusted deformation field (Cornell 1990; Davatzikos et al. 1996; Machado and Gee 1998; Gaser et al. 1999; Gaser et al. 2001; Borghammer et al. 2010). Of note, the DBM could not only provide the robust and reliable results concerning the association between the anatomical dynamics and neurobiological configurations but this method was also ideally suitable for the cross-sectional studies with specific regard of brain morphologies (Leow et al. 2006; Cardenas et al. 2007; Hua et al. 2008; Leow et al. 2009).

In this study, the high-resolution anatomical images were co-registered to the presupposed template by the B-Spline Free Form deformation algorithm driven by the entropy and were further normalized with same nonlinear transformation for capturing local deformations of regional changes (Studholme et al. 2001a, 2001b, 2003). To quantify the mathematical natures of local adaptation of deformations, the Jacobian determinant, which was used in gauge of the changes of flowing liquids or gases, was estimated for each voxel (Gaser et al. 2001). More details can be found in the SI method.

Surface-Based Morphometry

For in-depth comprehension on the morphological features of procrastination, we further leveraged the projection-based analysis (PBA) to characterize its brain neuroanatomical underpinning with the natures of surface-based morphometry, including CT and cortical folding (i.e., gyrification, local surface complexity and sulcus depth) (Dahnke et al. 2013). Here, the canonical preprocessing pipeline of surface mesh implemented in the CAT12 was executed: First, to overcome the drawback resulting from the misestimation of brain tissues due to asymmetrical iron concentration, the partial volume approach embedded in AMAP protocol was utilized for the segmentation (Dahnke et al. 2013); then, the CT was estimated as the absolute distance from the WM to its local maxima of the neighboring projective gray matter voxel (Dahnke et al. 2013); afterwards, the correction of SPHs was conducted to facilitate the compensation of topological obscure for the better estimation of the CT (Yotter et al. 2011a); furthermore, we reconstructed the spherical map of a cortical surface and handled the information concerning the partial volumes, sulcal blurring as well as sulcal asymmetries with the fast algorithm for the modified reparameterization of the local surface mesh (Yotter et al. 2011a); finally, the adaptive DARTEL algorithm was used in the spherical registration to calculate the sulcal depth and other surface-based shapes (e.g., gyrification and cortical surface complexity in 3D) (Ashburner 2007; Yotter et al. 2011b).

During the PBA, the absolute average curvature of cortical surface was extracted for the measure of gyrification (Luders et al. 2006). In addition, the FD was estimated for quantifying the cortical complexity (Yotter et al. 2011b) (see SI Method for details on these measures). In line with the suggestions derived from previous studies, the smooth process with Gaussian kernel of FWHM 15 mm was applied for the CT data, while the 20 mm for cortical folding data (Dahnke et al. 2013).

Quality Control

Given that the robustness and reproducibility of analysis could be heavily hampered by the critical quality of MRI images, we retrospectively scrutinized all the images after preprocessing with several cardinal parameters, including BWP noise, BWP bias, and RES resolution. For convenience of straightforward evaluation, these parameters were summed up to a weighted mean ranging from 0 to 100 points and were then ranked with 16 grades ranging from A+ to F (see SI for some examples). According to the empirical quantification of quality control (Gaser and Dahnke 2016), these images should be discarded from analysis in case the score was <60 or the rank was inferior than E+. As a result, three images were removed from date sets in the subsequent statistical analysis.

In addition, we visually checked the corresponding correlation matrix between all the volumes for remaining images. In principal, the high intracorrelation between them could be predominantly observed. Meanwhile, we found the acceptable data quality in our data sets according to the pattern of correlation matrix (see SI for examples). Likewise, we also illustrated the boxplot to intuitively determine the quality of these images, of which result showed the high homogeneity of our data. Finally, we combined the correlation matrix and estimated parameters of images to measure the Mahalanobis distance for quality checking, and the result indicated the high quality of our data as well.

Statistics

Behavioral Brain Configuration

In Sample 1 ($n = 242$), we drew on the VBM (i.e., GMV and GMD), DBM (Jacobian determinant [$|J|$]), and SBM (CT, gyrification index [ACC], and surface complexity [FD]) analysis to detect

the brain morphological dynamics of procrastination and further undertook the multilinear regression models to fit these patterns for procrastination. Taking the potential biases resulting from gender or other neurobiological factors on the measures of brain morphology and procrastination into account (Kulynych et al. 1994; Özer et al. 2009), gender, age, education, BMI, big-five personality traits, and total intracranial volume (TIV) were putted into the model as the covariates of no interests. To ensure the performance of this regression model, we undertook the intercorrelation analysis to correlate these covariates to targeting variable for the simple diagnosis of the co-linearity of this model, with $r > 0.30$ and $P < 0.05$ for the critical co-linearity (Liu et al. 2013). Results indicated that no co-linearity between PPS and these covariates was observed (gender, $r = 0.051$, $P = 0.451$; ages, $r = -0.033$, $P = 0.629$; education, $r = -0.011$, $P = 0.869$; BMI, $r = 0.126$, $P = 0.061$; conscientiousness, $r = 0.090$, $P = 0.182$; extraversion, $r = -0.057$, $P = 0.403$; neuroticism, $r = -0.043$, $P = 0.529$; agreeableness, $r = -0.038$, $P = 0.574$; openness, $r = 0.065$, $P = 0.333$; TIV, $r = -0.027$, $P = 0.693$). To ensure the balance between false-positive and false-negative results, an explicit mask with absolute threshold of 0.2 was applied to restrict the searching volumes (http://www.cs.ucl.ac.uk/staff/g.ridgway/masking/; (Ridgway et al. 2009). Likewise, the nonparametric Threshold-Free Cluster Enhancement (TFCE) correction with cluster-level $P < 0.05$ was adopted to alleviate the potential bias due to the multiple comparisons in the whole brain. This algorithm has been proven as a rigorous correction for the efficaciously limited false-positive rates in the nonstationary neuroimaging data (Smith and Nichols 2009; Nenadic et al. 2015). The threshold of statistical significance was set at $P < 0.001$ without correction to capture voxels or surfaces that were correlated with the procrastination, and then, we identified these surviving local dynamics of brain morphology after TFCE correction (TFCEC).

Brain-Behavioral Configuration

In order to acknowledge the reliability of these findings concerning the association between brain morphological characteristics of these brain areas and procrastination, we extracted the GMV, GMD, and J values of these significant clusters derived in last analysis from processed anatomical images using the MATLAB script "get_totals" (http://www.cs.ucl.ac.uk/staff/g.ridgway/vbm/get_totals.m) to correlate with behavioral procrastination scores in independent Sample 2 ($n = 215$). Likewise, the surface-based atlases generated from the FreeSurfer protocol was utilized to extract these values concerning the CT and cortical folding (i.e., gyrification and surface complexity) for the correlation analysis (Desikan et al. 2006; Destrieux et al. 2010). Here, the nonparametric Spearman partial correlation model was performed owing to its robustness even though the outliers presented in the dataset, while the gender, age, education, BMI, big-five personality trait, and TIV were recognized as covariates of no interests. Aside from estimation of the correlation coefficient per se, the 95% confidence interval (CI) was evaluated with the bootstrapping procedure (with 5000 bootstrap samples).

Prediction for Procrastination with Linear Regression Model

For the investigation regarding the predictive role of brain morphological dynamics on procrastination, the linear multiple step-wise regression model was built up leveraging the estimation of OLS method for the sake of the regression of PPS scores (dependent factor) against GMV, GMD, CT, gyrification, and cortical complexity (independent factors) in the independent Sample 3 ($n = 221$). Obviously, we hardly denoted all the possible mixed regression models here but provided the most ideal model that we expected as below:

$$y = \sim \beta_0 + \beta_1 \times \mathrm{GMV} + \beta_2 \times \mathrm{GMD} + \beta_3 \times J + \beta_4 \times \text{Cortical thickness} + \beta, \times \mathrm{ACC} + \beta_6 \times \mathrm{FD} + \varepsilon$$

where each β indicated the partial regression coefficient and ε served as the residual. To obtain the optimal model for elucidating the predictive role of brain morphological dynamics on procrastination, the correlation matrix (R) of all factors in the regression model was generated, and the first independent variables were selected to enter the model according to its partial regression sum of squares (u, see SI Method). In this study, the final model would be determined with the Bayesian information criterion (BIC) and the Akaike information criterion (AIC). Above analyses were all implemented by the functions of "lm.pred," "step" and "drop" in the R package (version: x64 3.4.1; https://www.r-project.org/).

As it is well known, even though this model of OLS can be considered potently productive for accurateness, it is still remains some critical drawbacks that can be hardly tackled: (1) OLS was designed as a unbiased statistic, but multiple co-linearity of independent variables would result in the out-of-control variance, and thus, the performance of this model would be biased at the expense of lower predictive parameters and (2) in terms of interpretation of predictive model, it is better to constrain the free or alternative parameters in the OLS model—if in this case—the model would be interpretative and accurate. Thus, to address this concern well, previous studies applied the Penalty function for the feature selection and estimations of free parameters, particularly in the LASSO algorithm (Tibshirani 1996, 2011). LASSO algorithm for the regression analysis was raised by Tibshirani (1996), and was used for the shrinkage estimate leveraging L1 regularized penalty term. Regression model of LASSO would utilize the L1 norm to constrain the model parameters (i.e., β) and thus result in these parameters to be less and further compress parameters—whose absolute values are close to 0—as 0 straightforward. In this vein, this model is not only beneficial from the less parameters to ameliorate the interpretation but also tailors this model for the robustness. In other words, owing to the advances of the LASSO algorithm for compressed sensing, a L1-LASSO regression model was drawn on estimations of these parameters for our predictive fits.

Prediction for Procrastination with Bayesian Estimation Model

Furthermore, the Bayesian model estimation of regression was performed as well. As was well known to all, the over-reliance on conventional NHST has largely impeded the reproducibility of outcomes in many profiles of psychology during the last decade (Anderson et al. 2000; Gliner et al. 2001; Wasserstein and Lazar 2016). Instead, the Bayes estimation based on the a priori information was increasingly advocated to replace the NHST due to its superior statistical properties, such as the liberal precondition, sensitive detection power, and the clear corroboration for null hypothesis (Benavoli et al. 2016; Nathoo and Masson 2016). Algorithm and equation for the estimations of the Bayesian factor can be found in the SI Method.

As indicated in the previous study (Wagenmakers et al. 2018), we accept the default prior width with revised Cauchy distribution provided by JASP software (version: x64 0.9.0.1; https://jasp-stats.org; JASP team 2017). All the variables, which were permitted to enter this optimal model, were utilized as the a posteriori evidence in the Bayesian regression model for probing the adaptive prediction model.

Prediction for Procrastination with Machine Learning

Owing to the predominant capability on the generalization for new data in the prediction model yielded by machine learning, the epsilon-insensitive SVR (EI-SVR) based on the kernel method of Gaussian radial basis function (RBF) was undertaken. Given considerations on the calculation of inner products of vectors ($\Phi(x_i)\cdot\Phi(x_j)$), all included variables were preprocessed for the scaling to the range [−1 1] with Min–Max normalization ($x* = x$-min/max-min) implemented in the Matlab 2016b (MathWorks Inc.) prior to the SVR analysis. What's more, this operation could also overcome the drawback that the smaller numeric ranges were prone to be predominantly obscured by the greater ones (Schoelkopf et al. 2002).

For the remarkably productive SVR analysis, the RBF kernel function was applied here. Unlike function of linear kernel, RBF could function on the nonlinear space with the high performance as well, which largely depended on the mappings of training samples into higher-dimensional Hilbert space so that the dual object function could be solved rapidly (Keerthi and Lin 2003). In addition, the advantages of RBF on the balance between precision of statistical approximation and complexity of hyperparameters as well as the less arithmetical difficulties drove this selection for kernel function (Schoelkopf et al. 2002; Vapnik 2002). Thus, to combine these parameters of penalty function (C and γ), RBF was conducted in this SVR analysis and highlighted its justification. It should be borne in mind that the accuracy of the SVR was determined by the overarching parameters (C and γ) of RBF to a large extent (Benoudjit 2002; Taouali 2018).

As a consequence, estimating and modulating C and γ in the level-one-out cross-validation (LOOCV) devoted to the crux in our next step. As recommended by Ozay et al. (2017), the fast grid search method (GS) was adopted for seeking the optimum parameters in this study (Ozay et al. 2017). GS served as an exhaustive searching strategy to capture the best one from all the possible candidates for penalty function, and it showed strikingly feasible properties in small and moderate data sets (Bao and Liu 2006; Ma and Zhang 2015). Notwithstanding that, this straightforward searching seemed to be naive for parameter optimization to some degree. According to an evolutionary algorithm outlined by Kennedy and Eberhart (1999), the searching approach concerning particle swarm optimization (PSO) algorithm was undertaken as well (Kennedy and Eberhart 1999). Contrary to GS, PSO devoted to approximations or heuristics for seeking global optimum solution with quick convergence, thus being practice and robust in the EI-SVR model (Hu 2002; Coelho 2010; Lin et al. 2010). Meanwhile, the LOOCV procedures were largely prevented from the potential overfitting and underfitting issues (Cawley and Talbot 2004). Ultimately, the pair of these parameters derived from the GS method was applied for the reoptimization of SVR model, whose performance in the prediction was best relative to other alternatives.

For assessing the corresponding statistical significance of these prediction models with SVR method, the permutation test was performed iterating 20 000 times implemented by using our self-made script (Cui et al. 2017; Liu et al. 2018). In each iteration, all normalized variables, including the dependent and independent factors, would be randomly extracted and were further rearranged as these factors beforehand. Then, SVR analysis would be subsequently used in each permutation for structuring the resubmitted statistics and its background distribution. Finally, the ratio of number of same prediction statistic occurring in the permutations on the total of permutations (20 000 times) was estimated for the statistical significance with correction.

All estimations concerning SVR were actualized in the Libsvm package (http://www.csie.ntu.edu.tw/~cjlin/libsvm/) with default settings of parameters except the C and γ of RBF (Chang and Lin 2011).

Table 2 Results for the whole-brain VBM analysis concerning which brain regions can significantly predict procrastination with GMV in the Sample 1

Brain regions	Location	BA	MNI coordinates			t value
			x	y	z	
Only +						
Insula	Left	47/48	−30	18	−15	3.89
Anterior cingulum cortex	Left	11	−6	42	2	3.66
PHC	Right	36	24	−6	−38	3.87
Only −						
Middle frontal gyrus, dlPFC	Left	46	−43	54	2	−2.09

Results

All raw data and files concerning results can be free to access at OSF (website: https://osf.io/kdtp2).

Behavioral Brain Configuration

VBM Analysis

To ascertain the neuroanatomical understructure of behavioral procrastination as to the local volumetric dynamic, whole-brain VBM analysis was performed to correlate the procrastination to the GMV and GMD of brain. Results demonstrated that procrastination had a significantly positive correlation with local GMV in left insula (peak MNI coordinate [mm]: −30, 18, −15), left anterior cingulate cortex (ACC, peak MNI coordinate: −6, 42, 2), and left PHC (peak MNI coordinate: 24, −6, −38), but it was negatively correlated to GMV of left middle frontal gyrus (dlPFC, peak MNI coordinate: −43, 54, −2) as well (see Table 2 and Fig. 1).

With regard to the alternation of local GMD, we revealed parallel scenario that procrastination was positively associated with GMD of both left ACC (peak MNI coordinates: −2, 31, 0) and right middle frontal gyrus (vmPFC, peak MNI coordinates: 4, 41, −13; see Table 3). The specific location of these brain regions was illustrated in Figure 2.

DBM Analysis

There were null findings in the DBM analysis after the TFCEC.

SBM Analysis

Cortical thickness. Owing to the sound sensibility of CT for description of the brain shape, we constructed the same model to examine associations between behavioral procrastination

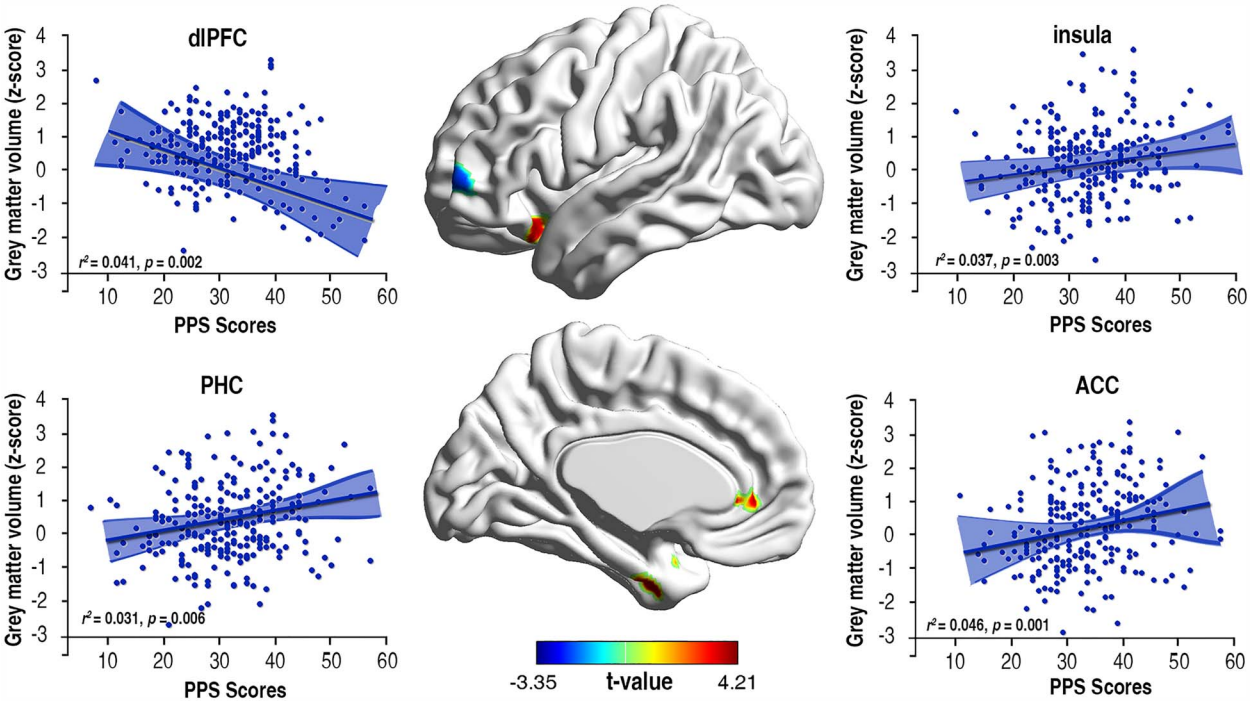

Figure 1. Brain maps and scatter plots for the correlation between the GMVs (z-scores) of significant clusters and the procrastination (PPS scores) in the Sample 1. The sagittal brain maps with both medial and lateral sides located at left hemisphere were mapped to the MNI152 space of the glass brain template. The shadow areas indicated the corresponding 95% CI for the estimated model.

Table 3 Results for the whole-brain VBM analysis concerning which brain regions can predict the procrastination with GMD in the Sample 1

Brain regions	Location	BA	MNI coordinates			t value
			x	y	z	
Only +						
Anterior cingulum cortex	Left	11/25	−2	31	0	6.58
Middle frontal gyrus, vmPFC	Right	11	4	41	−13	2.98

and CT. The results uncovered significantly positive association between procrastination and CT of bilateral OFC (left hemisphere, peak MNI coordinates: −4, 59, −20; right hemisphere, peak MNI coordinates: 6, 42, 2). Detailed information regarding these outcomes have been shown in Table 4 and Figure 3.

Cortical folding (gyrification and cortical 3D complexity). To further substantiate the brain shapes of procrastination, we performed the examination for the key link between procrastination and cortical folding including gyrification and surface complexity. Results showed that procrastination was positively correlated with cortical 3D complexity of bilateral OFC (left hemisphere, peak MNI coordinates: −4, 47, −16; right hemisphere, peak MNI coordinates: 9, 51, −2) (see Table 5 and Fig. 4). No significant association between the gyrification and procrastination was detected here.

Taken together, we built up the close link between procrastination and brain morphological dynamics in both brain size and brain shape. In detail, procrastination was negatively correlated to GMV of dlPFC, whereas positively associated with GMV of the insular, ACC, PHC and GMD of ACC, vmPFC, and CT/complexity of OFC.

Brain-Behavioral Reconfiguration

Given the increasing debates and controversy on reliability and reproducibility of the neuroimaging researches, we recruited the independent sample 2 (n = 215) further undertook the brain-behavioral analysis to cross-validate our results.

VBM Analysis

As aforementioned, significant associations between GMV of left insula (MNI coordinates [−30, 18, −15]), ACC (MNI coordinates [−6, 42, 2]), PHC (MNI coordinates [24, −6, −38]), dlPFC (coordinates [−43, 54, −2]), and procrastination were identified in the Sample 1. Here, these clusters were further drawn as masks for the extraction of the GMV. Subsequently, these values of GMV calculated from masks were utilized for the proportional global scaling. Finally, we built second-level model for partial correlation between values of these corresponding masks and procrastination in independent sample 2, while age, gender, education, BMI, and big-five personality were used as the covariables of no interests. Encouragingly, all the significant outcomes could be replicated in independent sample 2: local GMV of the ACC (r = 0.226, P < 0.001; 95% CI: 0.105–0.349), PHC (r = 0.240, P < 0.001; 95% CI: 0.122–0.359), and insula (r = 0.191, P < 0.005; 95% CI: 0.068–0.323) was positively correlated with procrastination, whereas local GMV of dlPFC was negatively associated to procrastination (r = −0.195, P < 0.004; 95% CI: −0.341 to −0.032). The scatter plots for these correlations have been depicted in Figure 5A–D.

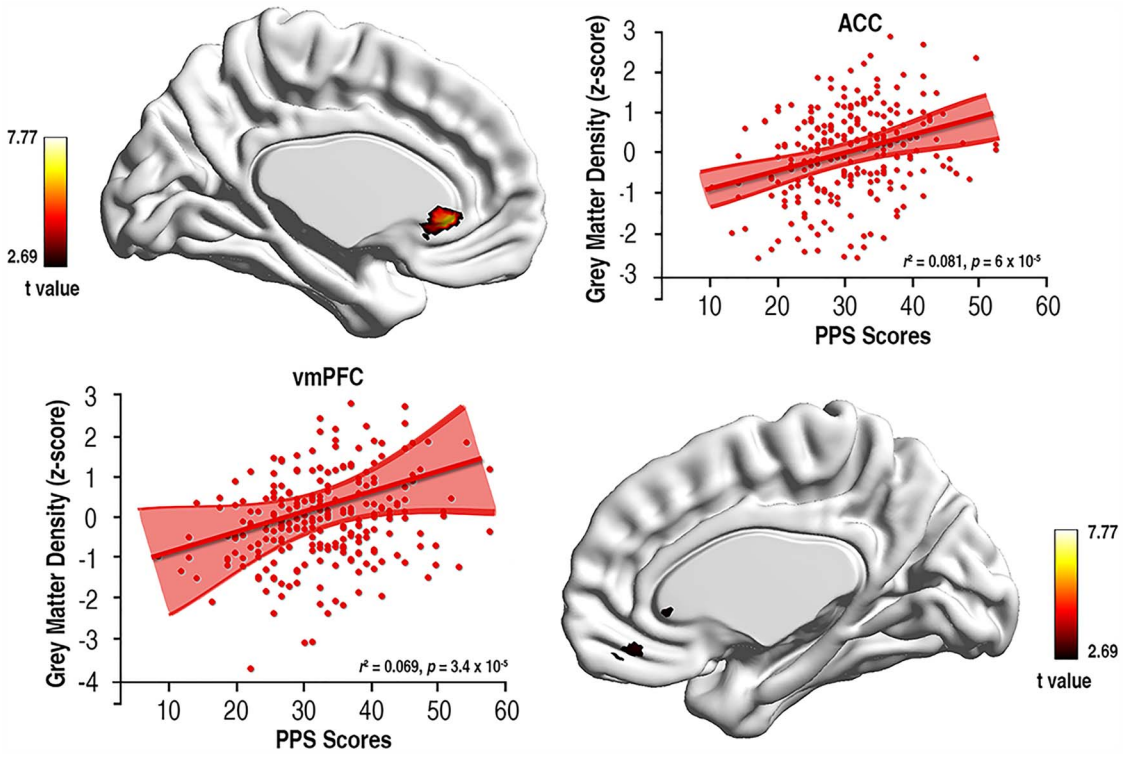

Figure 2. Brain maps and scatter plots for the correlation between the GMD (z-scores) of significant clusters and the procrastination (PPS scores) in the Sample 1. The sagittal brain maps with left medial and right medial sides were, respectively, mapped to the MNI152 space of the glass brain template. The shadow areas indicated the corresponding 95% CI for the estimated model.

Table 4 Results for the whole-brain SBM analysis concerning which brain regions can significantly predict procrastination with CT in the sample 1

Brain regions	Location	BA	MNI coordinates			*t* value
			x	y	z	
Only +						
Medial, OFC	Left	11/12	−4	59	−20	4.36
Medial, OFC	Right	11/12	6	42	2	4.01

The parallel results were found in this brain-behavioral reconfiguration as well: the significantly positive correlation between the GMD of left ACC ($r = 0.317$, $P < 0.001$; 95% CI: 0.210–0.421), vmPFC ($r = 0.318$, $P < 0.001$; 95% CI: 0.216–0.426), and procrastination was verified in the Sample 2 (see Fig. 5E,F).

SBM Analysis

Cortical thickness. Here, the independent multiscale atlases were concatenated to produce the mask of brain surfaces linking to procrastination, namely Desikan–Killiany atlas and Destrieux atlas. In the Sample 1, bilateral OFC (left hemisphere, MNI coordinates [−4, 59, −20]; right hemisphere, MNI coordinates [6, 42, 2]) was identified as the targeting brain regions for the explanation of neuroanatomical substrate underlying procrastination.

According to the automatic matching recognition implemented in the CAT toolbox, the masks of these significant brain surfaces were constrained in the vicinity of "medial/OFC" area of Desikan–Killiany atlas and 31 areas (rectus and suborbital sulcus) of Destrieux atlas. In this vein, these areas were further conducted as masks to make correlation between CT of brain surface and the procrastination in another independent sample for the sake of identification of the reproducibility of our findings. Finally, the partial correlation model was performed to examine this association.

Likewise, the significant positive correlations between CT of bilateral OFC and procrastination were replicated in independent sample 2 as well, irrespective of which masks of atlases were adopted (OFC [medial/OFC] of Desikan–Killiany atlas: r [left] = 0.192, $P < 0.005$, 95% CI: 0.068–0.320; r [right] = 0.163, $P < 0.05$, 95% CI: 0.026–0.304; OFC [31 area/rectus and suborbital sulcus] of Destrieux atlas: r [left] = 0.244, $P < 0.001$, 95% CI: 0.108–0.357; r [right] = 0.207, $P < 0.005$, 95% CI: 0.074–0.326) (see SI Results, Supplementary Fig. 7).

Cortical folding. To further examine the robust linking of dynamics of cortical surfaces on procrastination, we made use of partial correlation model for brain-behavioral reconfiguration regarding the cortical folding (i.e., cortical complexity) in Sample 2 for the validation of these findings. As aforementioned, the increased cortical complexity in bilateral OFC (left hemisphere, MNI coordinates [−4, 47, −16]; right hemisphere, MNI coordinates [9, 51, −2]) was positively correlated with procrastination. Interestingly, we found the significantly positive correlation between cortical complexity in the masks of bilateral OFC derived from Desikan–Killiany/Destrieux atlas and the procrastination, respectively (OFC [medial/OFC] of Desikan–Killiany atlas: r [left] = 0.189, $P < 0.005$, 95% CI: 0.043–0.320; r [right] = 0.145, $P < 0.05$, 95% CI: 0.010–0.272; OFC [70 area, suborbital sulcus] of Destrieux atlas: r [left] = 0.217, $P < 0.001$, 95%

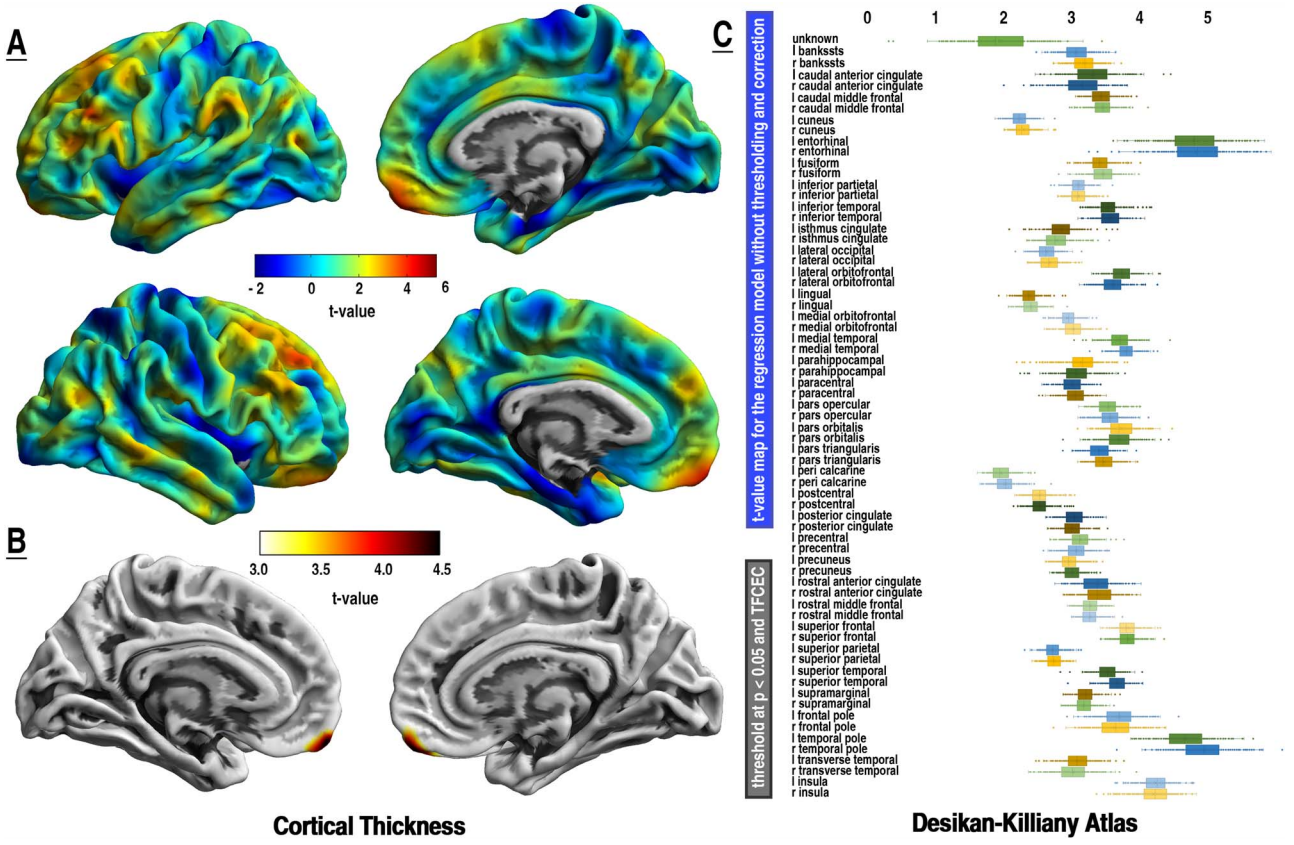

Figure 3. Brain spatial pattern for the parameter statistical map of *t*-values without thresholding procedures (*A*) and with threshold at the $P < 0.05$ of TFCEC (*B*) and the boxplots for the CT (mm) of whole-brain surface parceled from the Desikan–Killiany atlas of FreeSurface protocol (*C*). l = left hemisphere; r = right hemisphere.

Table 5 Results for the whole-brain SBM analysis concerning which brain regions can significantly predict procrastination with cortical folding in the Sample 1

Brain regions	Location	BA	MNI coordinates			*t* Value
			x	y	z	
Cortical complexity Only +						
Medial, OFC	Left	11, 12	−4	47	−16	3.89
Medial, OFC	Right	11, 12	9	51	−2	3.73

CI: 0.066–0.357; r [right] = 0.195, $P < 0.005$, 95% CI: 0.059–0.325) (see SI Results, Supplementary Fig. 8).

All in all, this brain-behavioral reconfiguration confirmed theses results of the significant association between volumetric features of brain morphology (i.e., GMV of the dlPFC, PHC, insular, ACC, and GMD of ACC, vmPFC, and CT/complexity of OFC) and procrastination in Sample 2. These findings have largely acknowledged the high reproducibility of this study. Such procedures potently preserved from potential risk of double dipping as well.

Prediction of Brain Morphology for Procrastination

Step-Wise Multiple Linear Regression Model

To obtain further insights into predictive role of brain morphological dynamics on the procrastination, the step-wise regression analysis was utilized to fit the model for dependent variable "scores of the procrastination" on independent variables including GMV of insula, GMV of ACC, GMV of PHC, GMV of dlPFC, GMD of ACC, GMD of vmPFC, CT of bilateral OFC, and the cortical complexity in bilateral OFC. Given the requirement for statistical benchmark of the regression model (Nelder and Wedderburn 1972; Pike et al. 1981; Cornell 1990), we utterly scrutinized the shape of data distribution for all variables with Kolmogorov–Smirnov test and Shapiro–Wilk test to determine whether it was corresponding to Gaussian distribution prior to the estimation of this model. Encouragingly, all the candidates were observed without significant skew on the Gaussian distribution (see Supplementary Table 1). For wider comprehension, we further provided informative details including range, mean, skewness, and kurtosis for all variables in Table 6.

Thus, all variables would be putted into the initial multiple regression model. Here, the entered criterion of stepwise process was defined with probability of $F \leq 0.05$ for each independent variable, whereas one would be rejected into the model in case of the probability of $F \geq 0.10$ for dependent variable. Afterwards, the step-wise iteration would automatically stop until no one could fit this criterion. Finally, GMV of dlPFC, GMV of PHC, GMV of insula, GMD of ACC, CT of right OFC, and cortical complexity in left OFC were available to enter the multiple regression model for explanation on the procrastination. The final model (Model VI) that encapsulated above six variables was captured as the best model (AIC = 853.45; BIC = 877.05) to significantly predict procrastination with account for 25.1% of total variance in dependent variable (adjust $R^2 = 0.251$, F(6,

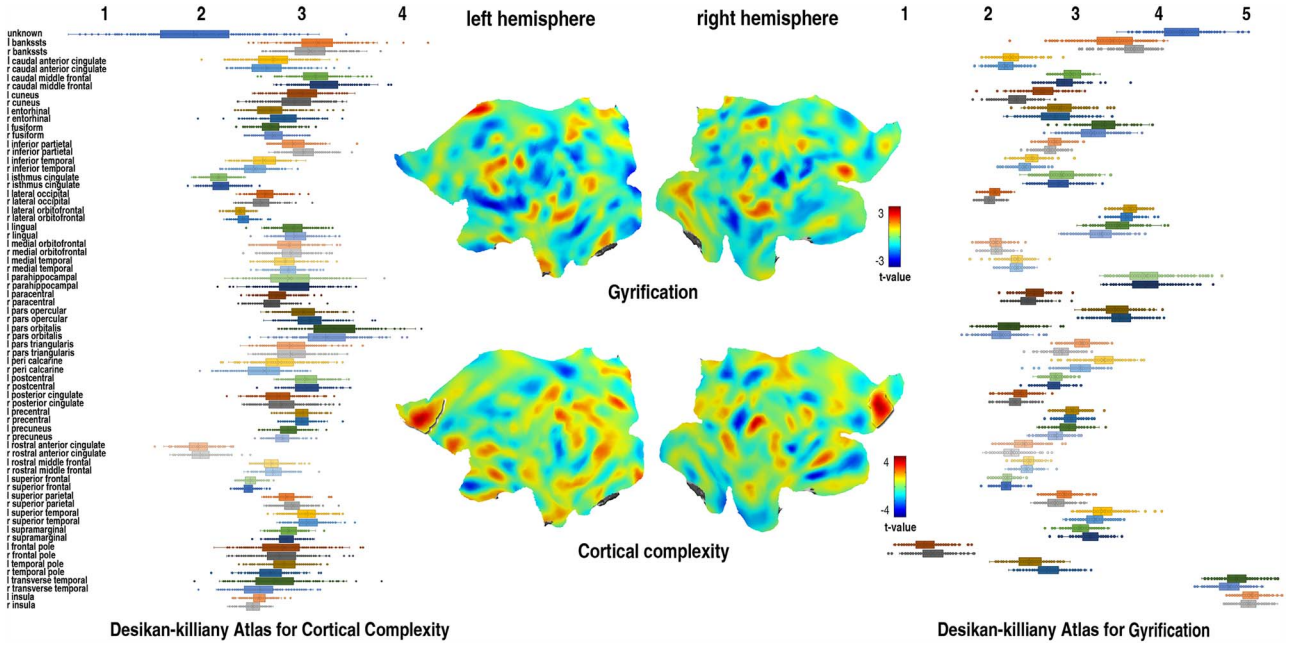

Figure 4. Flatmaps for the prediction of significant surfaces on the procrastination (middle panel) and boxplots for the distributions of cortical complexity (left panel) and gyrification (right panel) derived from Desikan–Killiany atlas in the Sample 1. These significant brain surfaces at $P < 0.05$ with Free-Threshold Cluster Enhancement correction devoting to predict procrastination are highlighted with bulge.

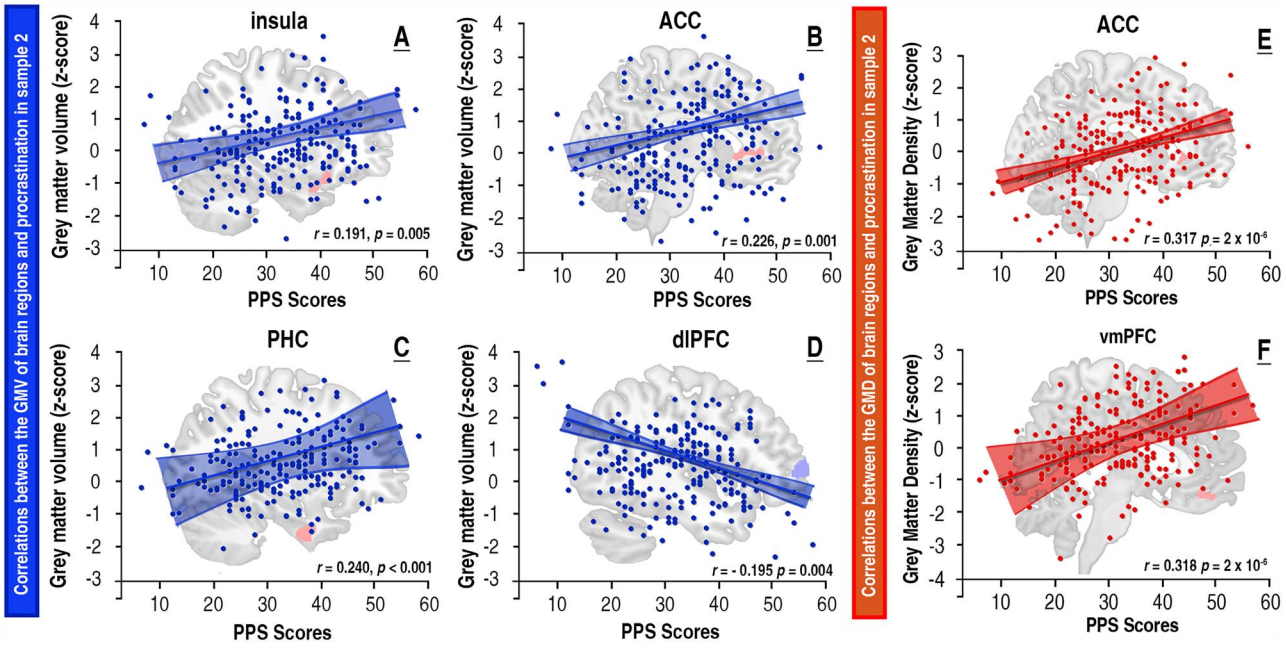

Figure 5. Scatter plots for the correlations between procrastination (PPS scores) and the GMVs (z-scores) of these significant clusters (*A–D*) and GMVs (z-scores) of those significant brain regions (*E,F*) in the Sample 2. All the values (i.e., GMV and GMD) of brain regions were extracted with the generated masks. Specific location of these brain regions in the mask was visualized behind corresponding scatter plot via the sagittal maps superimposed in MNI152 space. The shadow areas indicated the corresponding 95% CI for the estimated model.

214) = 13.282, $P < 0.001$; $b_{[GMD\_ACC]} = 0.237$, $t = 3.977$, $P < 0.001$; $b_{[Complexity\_l\_OFC\_2009s]} = 0.124$, $t = 2.023$, $P < 0.05$; $b_{[Pro\_GMV\_dlPFC]} = -0.377$, $t = -5.302$, $P < 0.001$; $b_{[Pro\_GMV\_PHC]} = 0.232$, $t = 3.145$, $P < 0.005$; $b_{[R\_OFC\_2009s]} = 0.132$, $t = 2.227$, $P < 0.05$; $b_{[Pro\_GMV\_Insula]} = 0.159$, $t = 2.008$, $P < 0.05$). Details concerning all models have been sorted in the SI Results (see Supplementary Table 2). Furthermore, the L1-LASSO regression model obtain highly parallel findings to substantiate the reliability of predictive role of these brain morphological dynamics to procrastination (Model 6 $R^2 = 27.3\%$; $df = 7$; step = 6; Rss = 10 647; Cp = 7.00; $\beta_{[GMD\_ACC]} = 154.51$, $\beta_{[GMD\_Insular]} = 17.38$, $\beta_{[GMD\_PHC]} = 16.33$, $\beta_{[Complexity\_l\_OFC\_2009s]} = 5.80$, $\beta_{[GMV\_dlPFC]} = -45.44$, $\beta_{[CT\_r\_OFC\_2009s]} = 1.88$) (see more details in SI Results). In short, the findings derived from this predictive model underscored a vital

Table 6 Results of Bayesian factor model for the step-wise multiple linear regression

	P (M)	P (M|data)	Bayes factor$_M$	Bayes factor$_{10}$	Error %
Model I	0.500	0.500	1.000	6189.331	1.61×10^{-4}
Model II	0.250	9.041	40.692	84406.243	0.003
Model III	0.125	0.838	36.158	468832.197	0.002
Model IV	0.063	0.892	124.394	364092.079	0.006
Model V	0.031	0.573	41.567	565831.240	0.004
Model VI	0.016	0.284	24.961	742488.911	0.002

Table 7 Summaries of the findings across the GMV, GMD, CT, and cortical complexity (3D CC)

	GMV	GMD	CT (mm)	3D CC
Self-control	dlPFC ↓	–	–	–
	ACC ↑	ACC ↑	–	–
Emotional process	Insular ↑	–	OFC ↑	OFC ↑
	–	–	OFC ↑	OFC ↑
Episodic prospection	PHC ↑	vmPFC ↑	–	–
	–	–	–	–

indication that GMV of dlPFC, GMV of PHC, GMV of insula, GMD of ACC, CT of right OFC, and cortical complexity in left OFC could be allowed for prediction of procrastination. There was no significance for other brain morphological dynamics, thus indicating denying them to adjust this prediction model.

Bayesian Estimation Model

Furthermore, as we briefly reviewed in Introduction section, to resolve potential biases of false-positive stemming from NHST, we conducted the Bayes factor analysis that has been adopted previously to provide more robust evidence to examine the predictive model. According to the requirement for the Bayes analysis, the prior width of Bayes factor was evaluated with the default parameters embodied in JASP (Cauchy distribution, $r = 0.354$). Likewise, GMV of dlPFC, GMV of PHC, GMV of insula, GMD of ACC, CT of right OFC, and cortical complexity in left OFC were allowed to enter the regression model with sound statistical effects (Bayesian factor (BF)$_{[GMD\_ACC]} = 6179.331$; $BF_{[Complexity\_l\_OFC\_2009s]} = 32.524$; $BF_{[Pro\_GMV\_dlPFC]} = 10.989$; $BF_{[Pro\_GMV\_PHC]} = 4.040$; $BF_{[R\_OFC\_2009s]} = 6.850$; $BF_{[Pro\_GMV\_Insula]} = 3.053$). Encouragingly, we obtained the similar findings concerning the predication of these variables on procrastination in the Bayesian linear multiple model: The evidence is to support that these brain morphological dynamics could significantly predict the procrastination, which was much more 468 832 times stronger than null model in the light of those posteriori information ($BF_{10} = 468832.197$, $BF_M = 0.002$, Error = 0.002%). More information regarding all the six models were documented in Table 6 in detail.

As reported in prior studies, the Bayes factors (BF_{10}) was considered as the strength of evidence for alternative model, with <3 for anecdotal supports, 3–10 for moderate supports, 10–30 for strong supports, 30–100 for very strong supports, and >100 for decisive evidence (Jeffreys 1998); Wagenmakers et al. 2018). As a consequence, these outcomes indicated the remarkable prediction of above brain structural substrates for procrastination, including GMV of dlPFC, GMV of PHC, GMV of insula, GMD of ACC, CT of right OFC, and cortical complexity in left OFC.

ES-SVR Embodied in Machine Learning Model

Finally, owing to better generalization performance of SVR of machine learning algorithm relative to above, EI-SVR, in conjunction of RBF kernel, was undertaken to prediction of above neuroanatomical characteristics for behavioral procrastination. Compared to searching strategy for optimal PSO algorithm, the fast grid method showed better machine performance on estimation for C and γ of RBF. Thus, the parameter settings of SVR model was undergone with the results derived from GS searching ($C = 9.189$, $\gamma = 0.108$; see SI Results, Supplementary Fig. 9). Our findings showed that these brain features could significantly predict procrastination ($r^2 = 0.629$, mean square error (MSE) = 0.001, $P = 0.011$, permuted with 20 000 times). Thus, this outcome encouraged us to draw the conclusion that comprehensive dynamics of both brain size (GMV of dlPFC, Insular and PHC, GMD of ACC) and brain shape (CT and complexity of OFC) could predict procrastination accurately.

Sum-Up in the Network-Based Insights

On balance, to gain all-round insights into the neural morphological dynamics of procrastination, the behavioral-brain analysis and the test–retest brain-behavioral examination were undertaken, respectively. Results converged in this line that procrastination was negatively correlated with GMV of dlPFC but was positively associated to GMV of ACC, insula, PHC, GMD of ACC, vmPFC, CT of OFC, and complexity of OFC (see Table 7). Furthermore, deriving from the prediction estimations (e.g., machine learning), the predictive roles of GMV of dlPFC, insula, PHC, GMD of ACC, and CT/complexity of OFC on procrastination have been ascertained in robust (see Fig. 6A). In this vein, as we introduced beforehand these findings on the behavioral brain configuration highlighted the underlying dynamics of insular, OFC playing hub roles in the emotional regulation system, alternations of the dlPFC, ACC taking part in the self-control, and features of PHC, vmPFC touching upon the function of the episodic future thinking for the procrastination. In other words, overall these outcomes have indicated us to advance a model to account the core components of the procrastination in the brain morphological subnetworks, namely self-control network, emotional regulation network, and the episodic future prospection network (see Fig. 6B).

Discussion

Brief Summary

This study recruited a large sample ($n = 688$) to explore the brain morphological dynamics of procrastination by using the robust measures for brain volumes (size) and cortical surfaces (shape). Our findings showed that the GMV of dlPFC was negatively correlated to procrastination, while the GMV of ACC, insular, PHC, and GMD of ACC, OFC, and CT/complexity of OFC were positively correlated to procrastination. Encouragingly, these findings could be cross-validated in independent sample 2. Furthermore, predication analysis demonstrated that these brain morphological features (i.e., GMV of dlPFC, PHC, insular, GMD of ACC, and CT/complexity of OFC) were the robust predictor for the procrastination. In this vein, these outcomes converged to this line that the dynamics of dlPFC, ACC responsible for self-control regulation, insular, ACC involved in emotional processes and vmPFC, and PHC taking part in the episodic future thinking could be recognized as neural understructure of procrastination comprehensively. In conclusion, this study concerning the brain morphological dynamics of procrastination elucidated

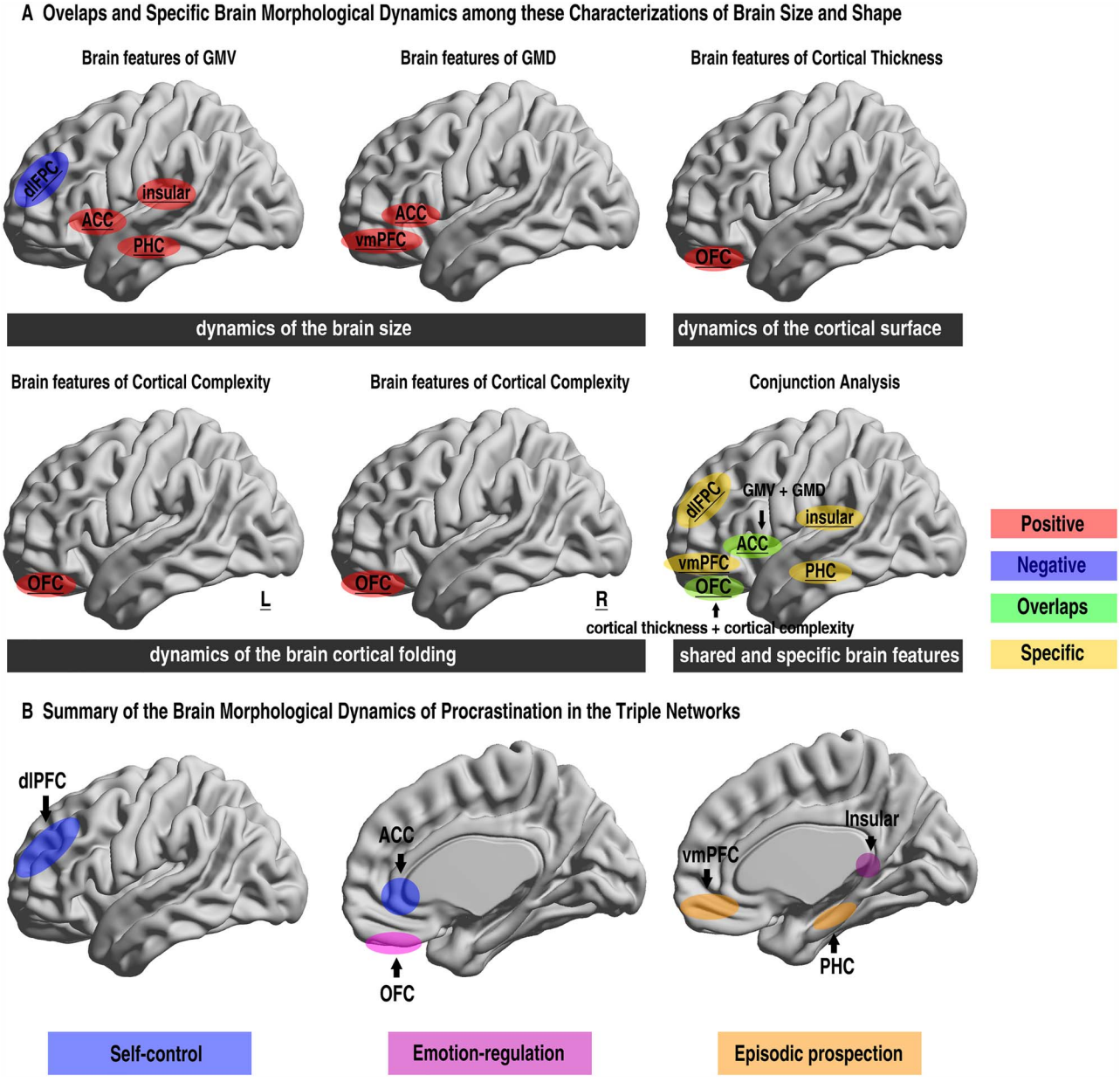

Figure 6. Summary of this study for major findings among all the brain morphological dynamics. (*A*) Identified common and separate features in the brain morphology across brain size, cortical surface, and cortical folding. The color of the background indicates the correlations of these clusters on the procrastination expecting the last one. Red represents the positive correlation, whereas the blue shows the negative association. (*B*) The triple brain network of the procrastination was proposed according to above results. Each color of the background is corresponding to the specific system (network).

the robustly predictive role of self-control system, emotional regulation system, and episodic prospection system for procrastination, which provided the novel comprehension for biobehavioral underpinning of procrastination and further clarified the potential targets useful for intervention.

Core Role of These Triple Brain Systems

Self-Control Network

As aforementioned, the GMV of dlPFC and the GMD of ACC were significantly correlated to procrastination, which were consistently encapsulated into the brain self-control network. A considerable round of studies indicated that self-control has been widely considered as most robust portrait for the core component of procrastination (Steel 2007; Zhang et al. 2019b). Previous studies indicated that self-control governed the irrational pursuit toward the short-sighted "comfort" of task-free instead of the task engagement, thus driving procrastination straightforward (Eerde 2003; Gustavson et al. 2014; Wu et al. 2016). In addition, this idea was in line with the psychological model concerning the self-imposed deadline for task (Ariely and Wertenbroch 2002). They accounted the nature of procrastination as the failure of self-control for precommitment on this task. Emerging studies provided evidences robust to evince that the self-control for impulsive decisions toward intertemporal decision can heavily constrain the undue delay discounting for

future profits (Zhang and Feng 2019; Zhang et al. 2019b). As to the role of self-control for procrastination, researchers do believe that it would work for the subjective evaluation of future outcome, thus determining the expectancy of outcome (utility) (Steel 2007; Zhang et al. 2019b). The dlPFC was known as the hub for regulation of self-control for the long time (Hare et al. 2009). As the hub of self-control system, the function of dlFPC was selectively responsible for the top–down cognitive control for downstream signals (MacDonald, 3rd et al. 2000; Hare et al. 2009; Figner et al. 2010).

In other regard, self-control system in brain pattern has been widely adopted to expand for ACC as well. Ample evidences have clarified the role of ACC as conflict monitoring and reinforcement learning of the error signals in the processes of decision (MacDonald, 3rd et al. 2000; Botvinick 2007; Pine et al. 2009; Peters and Büchel 2011). Even though the ACC seemed to be hard to probe self-control directly, it would be in charge for the modulation of cognitive resources in favor of processes of the self-control remarkably (Botvinick 2007; Marco-Pallarés et al. 2010). Intriguingly, in terms of brain intrinsic functional network, the dlPFC and ACC were observed as an integrative system (network), called cognitive control network (Bae et al. 2006; Alexopoulos et al. 2012). More vulnerabilities in neuropsychiatric illnesses pertaining to the deficits of cognitive self-control were frequently reported in low-performance of this unit (Alexopoulos et al. 2012; Whelan et al. 2012). Naturally, it was reasonable and justified to perceive dlPFC and ACC into this more comprehensive self-control network as brain morphological benchmark for core component of procrastination, with disturbance of self-control network for procrastination.

Emotional Regulation Network

As far as the core components of procrastination were considered, emotional processes for the engagements of task should be noticed in the brain morphological features. Fortunately, this study found the positive correlation between GMV of insular, GMD of OFC, and CT/complexity of OFC and procrastination, and these regions fitted well with theoretical account. Taking into account that major reason of procrastination was negative emotional feedback for the task, how to induce or regulate emotional processes for intended courses was increasingly becoming the crux that should be tackled (Ackerman and Gross 2005; Steel 2007).

Till now, emotion regulation theory raised by Sirois and Pychyl (2013) was considered as one of the most solid account for elucidating cognitive mechanism of procrastination (Sirois 2014a, 2014b). This model maintains this idea that individuals are more likely to postpone scheduled tasks in order to repair emotional depletion stemming from the task per se. In other word, to avoid short-term negative emotions resulting from the task, individuals would rather sacrifice long-term task rewards to experience well, thus rendering procrastination. Also, several lines of evidence have corroborated this explanation, showing predictive role of emotional regulation for procrastination (Pychyl et al. 2000; Lavoie and Pychyl 2001; Myrick 2015; Eckert et al. 2016). All in all, the current study provided neuroanatomical evidence sound reliable to substantiate this account straightforward.

Obviously, as the crucial subcortical region for the salience network, the insular played a cardinal role of social emotion and averseness on the task-evoked signals (Sridharan et al. 2008; Uddin 2015). Moreover, several lines of evidence substantiate this case straightforward that the insular had highly implicated to emotional downregulation and follow-up processes (Phan et al. 2005; Lindquist et al. 2012). Likewise, the function of OFC was considered to be comparable with insular (Davidson et al. 2000; Ochsner and Gross 2005). OFC was widely reported to engage in regulation for negative emotions and further in-depth processes toward re-evaluations (Kanai and Rees 2011; Petrovic et al. 2016). Literature of the affective neuroscience provided evidence to powerfully prove the role of OFC for emotional coding and regulation in a general brain network (Lindquist et al. 2012). In addition, the dysfunctions of OFC were regarded as the robust fingerprint for affective disruption, such as obsessive–compulsive disorder (Piras et al. 2013; Shaw et al. 2015; Fouche et al. 2017). These findings derived from previous literature hinted this standpoint that both regions could be perceived into an integrated system called "emotion-regulation" network, which was specialized to emotional processes for the averseness in task engagements, with high-performance emotional regulation for less procrastination.

Episodic Prospection Network

In this study, GMV of PHC and GMD of vmPFC were together correlated to procrastination positively. Just like intertemporal decisions, procrastination could be also regarded as a future-orientation decision, which required individuals make a choices between "to do it now" and "to do it later." Thinking for the future serves to an integral function of human beings, which can be refined as a projection of self-cognition for the future events and its pre-experiences (Atance and O'Neill 2001). In this vein, it makes sense to attempt to delineate the mechanism of procrastination by performance of episodic future thinking. Even though it is still lack for a theoretical account to explain the episodic prospection as underlying component for procrastination, a robust body of studies has highlighted the role of such episodic future thinking toward future incentive for inhibition of procrastination (Daniel et al. 2013; Rebetez et al. 2016). As reviewed above, episodic future prospection was attested as cardinal component for the processes of procrastination in the task valuation (Zhang et al. 2019b). Typically, the episodic prospection toward future referred to a productive tactic allowed the constraint of undue discounts on the task future long-term profits, thus mitigating procrastination in the light of high evaluation for the task outcomes (Peters and Büchel 2010; Benoit et al. 2011; Daniel et al. 2013). PHC served as the hub of medial temporal lobe (MTL) to partake of the episodic memory and episodic future thinking (Okuda et al. 2003; Peters and Büchel 2010, 2011). Previous literature pertaining to organic brain damage indicated that the deficits of PHC in MTL circuit could result in prominently specific curb for the episodic memory of past experience and future-orientated episodic thinking (Race et al. 2011; Irish et al. 2013; Schacter et al. 2017).

Aside from this subcortical hub, as the high-order prefrontal topology, vmPFC functioned to the episodic future thinking as well, especially in future-focused and goal-oriented prospection (Bertossi et al. 2016; Bertossi et al. 2017). Unlike to retrospective details of pre-experiences in MTL, the overarching contributions of vmPFC to episodic future thinking were to yield more abstract imagination after self-referential processes for individuals per se (D'Argembeau 2013; Motzkin et al. 2014). In this vein, the engagements of vmPFC in episodic future thinking would do works to deliberate processes for the future task costs and outcomes leveraging the updated self-knowledge (experience) simulation, thus determining whether the task would be protracted (Bertossi et al. 2016; Bertossi et al. 2017). Thus, a sound

promising conjecture was advanced for this explanation here, which integrated PHC and vmPFC into the episodic prospection network to account the functions of future thinking for the procrastination (Andrews-Hanna et al. 2014). On balance, we drew the conclusion that procrastination could be attributed to maladaptive episodic future thinking for the task value since the brain morphological aberrant alternation in the brain episodic prospection network (i.e., PHC and vmPFC).

Limitations and Directions

One major concern regarding these findings of this study was that these outcomes rarely answered real-time processes of the procrastination giving a task. Future research leveraging the exquisite design for the task-related fMRI can potently extend the explanation of the theoretical account in the more specific details of the task processes of procrastination. Another limitation in this study involved the issue of the classifications of the procrastination using the machine learning. To extend these findings to a wider application, the procrastination can be encoded as the binary label for the diagnosis in the future. In addition, in this study, it should be warranted some cautions that the prediction of these brain morphological dynamics for procrastination implicated a statistical association but not actually causal pathways from neurobiological substrates to procrastination. In this vein, there was a promising aspect of future researches to reveal a practical causal pathway for understandings of procrastination. We do believe that the neurointervention—such as transcranial magnetic stimulation and transcranial direct current stimulation—can reap huge fruits for insights into causal identification in the future study.

Owing to the growing calls for the understandings of brain connectome, neurobehavioral underpinning can be not only described as the dysfunctions of single network but rather attributed to the connections or connectome of these brain subsystems (Sporns et al. 2005; Bassett and Sporns 2017). Although we can hardly delineate the interplay of these triple brain networks (systems) on the basis of this study, it still should be discussed here as the future directions. In this vein, it is more valuable to depict the procrastination in the network-connectome model, which would allow us to obtain some more powerful evidence as to how these core components work and interact with the processes of the procrastination. Recently, an investigation for the role of the interplay among brain intrinsic large-scale networks does pioneer this insight into the network-connectome facet: The connection of the Salience Network–Subcortical Network can predict the procrastination significantly (Su et al. 2018). Thus, the future researches can reap huge fruits from the examinations for the pattern of the interplay across these brain subsystems, namely self-control network, emotional regulation network, and episodic prospection network.

Conclusion

Here, we described the brain morphological dynamics of procrastination in terms of brain size and cortical surfaces, which showed the significant positive link of GMV in the insula, PHC, ACC and GMD of ACC, vmPFC, and CT/3D complexity of bilateral OFC to procrastination. On the other hand, the GMV of the dlPFC was negatively correlated to procrastination. Furthermore, we manifested the certainly predictive role of the specific brain neuroanatomical characteristics for procrastination, which included the GMV of dlPFC, PHC, insula, and the GMD in the ACC, as well as CT/3D complexity in the cluster of OFC. In conclusion, this study provided the first insights into all-around brain morphological dynamics of procrastination and promoted the understandings of the neural understructure of the procrastination in the triple brain subsystems, including self-control network, emotional regulation network, and episodic prospection network.

Supplementary Material

Supplementary data is available at *Cerebral Cortex* online.

Funding

National Natural Science Foundation of China (31571128, 31971026); Fundamental Research Funds for the Central Universities (SWU1809357).

Notes

All procedures performed in studies involving human participants were in accordance with the ethical standards of the IRB of the Southwest University and with the 1964 Helsinki declaration and its later amendments or comparable ethical standards. Informed consent was obtained from all individual participants included in the study. We sincerely appreciated to Yanchen Tang (Peking University, China; Shanghai Normal University, China) for his suggestion on the sorts of data, and Jiawei Xie (The University of Sheffield, UK) for his helps on the English polishing. *Conflict of Interest*: All the co-authors declare that they have no conflict of interest (corresponding at Tingyong Feng, No.2, Tian Sheng RD., Beibei, ChongQing 400715, China)

References

Alexopoulos GS, Hoptman MJ, Kanellopoulos D, Murphy CF, Lim KO, Gunning FM. 2012. Functional connectivity in the cognitive control network and the default mode network in late-life depression. *J Affect Disord*. 139(1):56–65.

Ackerman DS, Gross BL. 2005. My instructor made me do it: task characteristics of procrastination. *J Mark Educ*. 27:5–13.

Anderson MW, Peter K, John B, Laura A, Karl Z, Peter TF, Ravindranath D. 2010. Cortical thickness or grey matter volume? The importance of selecting the phenotype for imaging genetics studies. *Neuroimage*. 53:1135–1146.

Anderson DR, Burnham KP, Thompson WL. 2000. Null hypothesis testing: problems, prevalence, and an alternative. *J Wildl Manag*. 64:912–923.

Andrews-Hanna JR, Smallwood J, Spreng RN. 2014. The default network and self-generated thought: component processes, dynamic control, and clinical relevance. *Ann NY Acad Sci*. 1316:29.

Ariely D, Wertenbroch K. 2002. Procrastination, deadlines, and performance: self-control by precommitment. *Psychol Sci*. 13:219–224.

Ashburner J. 2007. A fast diffeomorphic image registration algorithm. *NeuroImage*. 38:95.

Ashburner J, Friston KJ. 2000. Voxel-based morphometry—the methods. *NeuroImage*. 11:805–821.

Ashburner J, Friston KJ. 2011. Diffeomorphic registration using geodesic shooting and gauss—Newton optimisation. *NeuroImage*. 55:954–967.

Atance CM, O'Neill DK. 2001. Episodic future thinking. *Trends Cogn Sci*. 5:533–539.

Atance CM, O'Neill DK. 2005. The emergence of episodic future thinking in humans. *Learn Motiv*. 36:126–144.

Bae JN, MacFall JR, Krishnan KRR, Payne ME, Steffens DC, Taylor WD. 2006. Dorsolateral prefrontal cortex and anterior cingulate cortex white matter alterations in late-life depression. *Biol Psychiatry*. 60:1356–1363.

Bao Y, Liu Z, editors. 2006. A fast grid search method in support vector regression forecasting time series. In *International Conference on Intelligent Data Engineering and Automated Learning* pp. 504–511. Springer, Berlin, Heidelberg.

Bassett DS, Sporns O. 2017. Network neuroscience. *Nat Neurosci*. 20:353.

Bauer IM, Baumeister RF. 2004. Self-regulatory strength. In: *Handbook of self-regulation*. 84–98. Spinger, London, UK.

Baumeister RF, Vohs KD. 2004. *Handbook of self-regulation: research, theory, and applications*. The Guilford Press. London, UK.

Benavoli A, Corani G, Demsar J, Zaffalon M. 2016. Time for a change: a tutorial for comparing multiple classifiers through Bayesian analysis. *J Mach Learn Res*. 18:2653–2688.

Benoit RG, Gilbert SJ, Burgess PW. 2011. A neural mechanism mediating the impact of episodic prospection on farsighted decisions. *J Neurosci*. 31:6771–6779.

Benoudjit N. 2002. Width optimization of the Gaussian kernels in radial basis function networks. *Proc Eur Symp Artif Neural Netw Apr*. 1:565.

Bertossi E, Candela V, De Luca F, Ciaramelli E. 2017. Episodic future thinking following vmPFC damage: impaired event construction, maintenance, or narration? *Neuropsychology*. 31:337.

Bertossi E, Tesini C, Cappelli A, Ciaramelli E. 2016. Ventromedial prefrontal damage causes a pervasive impairment of episodic memory and future thinking. *Neuropsychologia*. 90:12–24.

Besteher B, Squarcina L, Spalthoff R, Bellani M, Gaser C, Brambilla P, Nenadic I. 2017. Brain structural correlates of irritability: findings in a large healthy cohort. *Hum Brain Mapp*. 38:6230–6238.

Bin YU, Yue G, Liu H. 2007. The strength model of self-control. *Curr Dir Psychol Sci*. 16:351–355.

Borghammer P, K Ø Cumming P, Gjedde A, Rodell A, Hall N, Chakravarty MM. 2010. A deformation-based morphometry study of patients with early-stage Parkinson's disease. *Eur J Neurol*. 17:314–320.

Botvinick MM. 2007. Conflict monitoring and decision making: reconciling two perspectives on anterior cingulate function. *Cogn Affect Behav Neurosci*. 7:356–366.

Boyer P. 2008. Evolutionary economics of mental time travel? *Trends Cogn Sci*. 12:219–224.

Cardenas VA, Studholme C, Gazdzinski S, Durazzo TC, Meyerhoff DJ. 2007. Deformation-based morphometry of brain changes in alcohol dependence and abstinence. *NeuroImage*. 34:879–887.

Cardoso MJ, Melbourne A, Kendall GS, Modat M, Robertson NJ, Marlow N, Ourselin S. 2013. AdaPT: an adaptive preterm segmentation algorithm for neonatal brain MRI. *NeuroImage*. 65:97–108.

Cawley GC, Talbot NL. 2004. Fast exact leave-one-out cross-validation of sparse least-squares support vector machines. *Neural Netw*. 17:1467–1475.

Chang CC, Lin CJ. (2011). LIBSVM: A library for support vector machines. ACM transactions on intelligent systems and technology (TIST). 2:27.

Chung MK, Worsley KJ, Paus T, Cherif C, Collins DL, Giedd JN, Rapoport JL, Evans AC. 2001. A unified statistical approach to deformation-based morphometry. *NeuroImage*. 14: 595–606.

Cigdem O, Beheshti I, Demirel H. 2018. Effects of different covariates and contrasts on classification of Parkinson's disease using structural MRI. *Comput Biol Med*. 99:173–181.

Coelho LDS. 2010. Gaussian quantum-behaved particle swarm optimization approaches for constrained engineering design problems. *Expert Syst Appl*. 37:1676–1683.

Cornell J. 1990. Classical and modern regression with applications. *Technometrics*. 29:377–378.

Costa PT Jr, McCrae RR, Dye DA. 1991. Facet scales for agreeableness and conscientiousness: a revision of the NEO personality inventory. *Personal Individ Differ*. 12:887–898.

Costa PT, McCrae RR. 1992. Normal personality assessment in clinical practice: the NEO personality inventory. *Psychol Assess*. 4:5.

Cui Z, Su M, Li L, Shu H, Gong G. 2017. Individualized prediction of reading comprehension ability using gray matter volume. *Cereb Cortex*. 28:1–17.

D'Argembeau A. 2013. On the role of the ventromedial prefrontal cortex in self-processing: the valuation hypothesis. *Front Hum Neurosci*. 7:372.

D'Argembeau A, Renaud O, Van der Linden M. 2011. Frequency, characteristics and functions of future-oriented thoughts in daily life. *Appl Cogn Psychol*. 25:96–103.

Dahnke R, Yotter RA, Gaser C. 2013. Cortical thickness and central surface estimation. *NeuroImage*. 65:336–348.

Daniel TO, Stanton CM, Epstein LH. 2013. The future is now: reducing impulsivity and energy intake using episodic future thinking. *Psychol Sci*. 24:2339–2342.

Davatzikos C, Vaillant M, Resnick SM, Prince JL, Letovsky S, Bryan RN. 1996. A computerized approach for morphological analysis of the corpus callosum. *J Comput Assist Tomogr*. 20:88.

Davidson RJ, Putnam KM, Larson CL. 2000. Dysfunction in the neural circuitry of emotion regulation—a possible prelude to violence. *Science*. 289:591–594.

De Ridder DT, Lensvelt-Mulders G Finkenauer C Stok FM Baumeister RF. 2018. Taking stock of self-control: a meta-analysis of how trait self-control relates to a wide range of behaviors. Personality & Social Psychology Review An Official Journal of the Society for Personality & Social Psychology Inc, 16, 76.

Desikan RS, Segonne F, Fischl B, Quinn BT, Dickerson BC, Blacker D, Buckner RL, Dale AM, Maguire RP, Hyman BT *et al*. 2006. An automated labeling system for subdividing the human cerebral cortex on MRI scans into gyral based regions of interest. *NeuroImage*. 31:968–980.

Destrieux C, Fischl B, Dale A, Halgren E. 2010. Automatic parcellation of human cortical gyri and sulci using standard anatomical nomenclature. *NeuroImage*. 53:1–15.

Digdon NL, Howell AJ. 2008. College students who have an eveningness preference report lower self-control and greater procrastination. *Chronobiol Int*. 25:1029–1046.

Eckert M, Ebert DD, Lehr D, Sieland B, Berking M. 2016. Overcome procrastination: enhancing emotion regulation skills reduce procrastination. *Learn Individ Differ*. 52:10–18.

Eerde WV. 2003. A meta-analytically derived nomological network of procrastination. *Pers Individ Differ*. 35:1401–1418.

Escorial S, Román FJ, Martínez K, Burgaleta M, Karama S, Colom R. 2015. Sex differences in neocortical structure and cognitive performance: a surface-based morphometry study. *NeuroImage*. 104:355–365.

Esteban RFC, Ramírez A. 2014. Procrastination and demographic characteristics associated with college students. *TUMJ*. 72:113–120.

Farokhian F, Beheshti I, Sone D, Matsuda H. 2017. Comparing CAT12 and VBM8 for detecting brain morphological abnormalities in temporal lobe epilepsy. *Front Neurol*. 8:428.

Faul F, Erdfelder E, Buchner A, Lang AG. 2009. Statistical power analyses using G*power 3.1: tests for correlation and regression analyses. *Behav Res Methods*. 41:1149–1160.

Ferrari JR, Johnson JL, Mccown WG. 1995. *Procrastination and task avoidance: Theory, research, and treatment*. Springer Science & Business Media.

Figner B, Knoch D, Johnson EJ, Krosch AR, Lisanby SH, Fehr E, Weber EU. 2010. Lateral prefrontal cortex and self-control in intertemporal choice. *Nat Neurosci*. 13:538–539.

Fischl B, Rajendran N, Busa E, Augustinack J, Hinds O, Yeo BT, Mohlberg H, Amunts K, Zilles K. 2007. Cortical folding patterns and predicting cytoarchitecture. *Cereb Cortex*. 18:1973–1980.

Fouche JP, Du SP, Hattingh C, Roos A, Lochner C, Sorianomas C, Sato JR, Nakamae T, Nishida S, Kwon JS. 2017. Cortical thickness in obsessive-compulsive disorder: multisite mega-analysis of 780 brain scans from six centres. *Br J Psychiatry J Ment Sci*. 210:67.

Gaser C, Dahnke R. 2016. CAT—a computational anatomy toolbox for the analysis of structural MRI data. *HBM*. 2016:336–348.

Gaser C, Volz HP, Kiebel S, Riehemann S, Sauer H. 1999. Detecting structural changes in whole brain based on nonlinear deformations-application to schizophrenia research. *NeuroImage*. 10:107–113.

Gaser C, Nenadic I, Buchsbaum BR, Hazlett EA, Buchsbaum MS. 2001. Deformation-based morphometry and its relation to conventional volumetry of brain lateral ventricles in MRI. *NeuroImage*. 13:1140–1145.

Gerig G, Styner M, Shenton ME, Lieberman JA. (2001). Shape versus size: Improved understanding of the morphology of brain structures. In *International Conference on Medical Image Computing and Computer-Assisted Intervention* (pp. 24–32). Springer, Berlin, Heidelberg.

Gliner JA, Morgan GA, Leech NL, Harmon RJ. 2001. Problems with null hypothesis significance testing. *J Exp Educ*. 40: 250.

Gustavson DE, Miyake A, Hewitt JK, Friedman NP. 2014. Genetic relations among procrastination, impulsivity, and goal-management ability: implications for the evolutionary origin of procrastination. *Psychol Sci*. 25:1178–1188.

Gustavson DE, Miyake A, Hewitt JK, Friedman NP. 2015. Understanding the cognitive and genetic underpinnings of procrastination: evidence for shared genetic influences with goal management and executive function abilities. *J Exp Psychol Gen*. 144:1063.

Han X, Jovicich J, Salat D, Kouwe AVD, Quinn B, Czanner S, Busa E, Pacheco J, Albert M, Killiany R. 2006. Reliability of MRI-derived measurements of human cerebral cortical thickness: the effects of field strength, scanner upgrade and manufacturer. *NeuroImage*. 32:180–194.

Hare TA, Camerer CF, Rangel A. 2009. Self-control in decision-making involves modulation of the vmPFC valuation system. *Science*. 324:646–648.

Harriott JS, Ferrari JR, Dovidio JF. 1996. Distractibility, daydreaming, and self-critical cognitions as determinants of indecision. *J Soc Behav Pers*. 11:337–344.

Hu X, Eberhart RC. (2002). Adaptive particle swarm optimization: detection and response to dynamic systems. In *Proceedings of the 2002 Congress on Evolutionary Computation. CEC'02 (Cat. No. 02TH8600)* (Vol. 2, pp. 1666–1670). IEEE.

Hu Y, Liu P, Guo Y, Feng T. 2018. The neural substrates of procrastination: a voxel-based morphometry study. *Brain Cogn*. 121:11–16.

Hua X, Leow AD, Parikshak N, Lee S, Chiang MC, Toga AW, Jr JC, Weiner MW, Thompson PM. 2008. Tensor-based morphometry as a neuroimaging biomarker for Alzheimer's disease: an MRI study of 676 AD, MCI, and normal subjects. *NeuroImage*. 43:458–469.

Ide JS, Zhornitsky S, Hu S, Zhang S, Krystal JH, Li CSR. 2017. Sex differences in the interacting roles of impulsivity and positive alcohol expectancy in problem drinking: a structural brain imaging study. *Neuroimage Clin*. 14:750–759.

Irish M, Hodges JR, Piguet O. 2013. Episodic future thinking is impaired in the behavioural variant of frontotemporal dementia. *Cortex*. 49:2377–2388.

Jeffreys H. 1998. The theory of probability. *J Am Stat Assoc*. 17:135–136.

Kai JJ, Cesario J. 2015. How can preregistration contribute to research in our field? *CRSP*. 1:1–7.

Kanai R, Rees G. 2011. The structural basis of inter-individual differences in human behaviour and cognition. *Nat Rev Neurosci*. 12:231–242.

Keerthi SS, Lin CJ. 2003. Asymptotic behaviors of support vector machines with gaussian kernel. *Neural Comput*. 15:1667.

Kennedy J, Eberhart RC. 1999. *The particle swarm: social adaptation in information-processing systems*. UK: McGraw-Hill Ltd.

Knaus WJ. 2000. Procrastination, blame, and change. *J Soc Behav Pers*. 15:153.

Kulynych JJ, Vladar K, Jones DW, Weinberger DR. 1994. Gender differences in the normal lateralization of the supratemporal cortex: MRI surface-rendering morphometry of Heschl's gyrus and the planum temporale. *Cereb Cortex*. 4:107–118.

Kundu S, Kolouri S, Erickson KI, Kramer AF, McAuley E, Rohde GK. 2018. Discovery and visualization of structural biomarkers from MRI using transport-based morphometry. *NeuroImage*. 167:256–275.

Lavoie JA, Pychyl TA. 2001. Cyberslacking and the procrastination superhighway: a web-based survey of online procrastination, attitudes, and emotion. *Soc Sci Comput Rev*. 19:431–444.

Lee BK, Lessler J, Stuart EA. 2010. Improving propensity score weighting using machine learning. *Stat Med*. 29:337–346.

Leow AD, Klunder AD, Jack CR Jr, Toga AW, Dale AM, Bernstein MA, Britson PJ, Gunter JL, Ward CP, Whitwell JL *et al*. 2006. Longitudinal stability of MRI for mapping brain change using tensor-based morphometry. *NeuroImage*. 31:627–640.

Leow AD, Yanovsky I, Parikshak N, Hua X, Lee S, Toga AW, Jack CR Jr, Bernstein MA, Britson PJ, Gunter JL *et al*. 2009. Alzheimer's disease neuroimaging initiative: a one-year follow up study using tensor-based morphometry correlating degenerative rates, biomarkers and cognition. *NeuroImage*. 45:645–655.

Lin GH, Zhang J, Liu ZH. 2010. Hybrid particle swarm optimization with differential evolution for numerical and engineering optimization. *App Soft Comput J*. 10:1–12.

Lindquist KA, Wager TD, Kober H, Bliss-Moreau E, Barrett LF. 2012. The brain basis of emotion: a meta-analytic review. *Behav Brain Sci*. 35:121–143.

Liu J, Liao X, Xia M, He Y. 2018. Chronnectome fingerprinting: identifying individuals and predicting higher cognitive functions using dynamic brain connectivity patterns. *Hum Brain Mapp*. 39:902.

Liu L, Feng T, Chen J, Li H. 2013. The value of emotion: how does episodic prospection modulate delay discounting? *PLoS One*. 8:e81717.

Liu P, Feng T. 2017. The overlapping BRAIN region accounting for the relationship between procrastination and impulsivity: a voxel-based morphometry study. *Neuroscience*. 360:9–17.

Liu P, Feng T. 2019. The effect of future time perspective on procrastination: the role of parahippocampal gyrus and ventromedial prefrontal cortex. *Brain Imaging Behav*. 13:615–622

Luders E, Thompson PM, Narr KL, Toga AW, Jancke L, Gaser C. 2006. A curvature-based approach to estimate local gyrification on the cortical surface. *NeuroImage*. 29:1224–1230.

Lynch JG, Zauberman G. 2006. When do you want it? Time, decisions, and public policy. *J Public Policy Mark*. 25:67–78.

Ma X, Zhang Y. 2015. In: Wang Y Performance evaluation of kernel functions based on grid search for support vector regression. In *2015 IEEE 7th international conference on cybernetics and intelligent systems (CIS) and IEEE conference on robotics, automation and mechatronics (RAM)* (pp. 283–288). IEEE.

MacDonald AW 3rd, Cohen JD, Stenger VA, Carter CS. 2000. Dissociating the role of the dorsolateral prefrontal and anterior cingulate cortex in cognitive control. *Science (New York, NY)*. 288:1835–1838.

Machado AMC, Gee JC. 1998. Atlas warping for brain morphometry. *Proc SPIE Int Soc Opti Eng*. 3338:642–651.

Maingault S, Tzourio-Mazoyer N, Mazoyer B, Crivello F. 2016. Regional correlations between cortical thickness and surface area asymmetries: a surface-based morphometry study of 250 adults. *Neuropsychologia*. 93:350–364.

Mangin J-F, Riviere D, Cachia A, Duchesnay E, Cointepas Y, Papadopoulos-Orfanos D, Scifo P, Ochiai T, Brunelle F, Regis J. 2004. A framework to study the cortical folding patterns. *NeuroImage*. 23:S129–S138.

Manjón JV, Coupé P, Martí-Bonmatí L, Collins DL, Robles M. 2010. Adaptive non-local means denoising of MR images with spatially varying noise levels. *J Magn Reson Imaging*. 31: 192–203.

Marco-Pallarés J, Mohammadi B, Samii A, Münte TF. 2010. Brain activations reflect individual discount rates in intertemporal choice. *Brain Res*. 1320:123–129.

McCullough ME, Willoughby BL. 2009. Religion, self-regulation, and self-control: associations, explanations, and implications. *Psychol Bull*. 135:69.

Motzkin JC, Philippi CL, Wolf RC, Baskaya MK, Koenigs M. 2014. Ventromedial prefrontal cortex lesions alter neural and physiological correlates of anticipation. *J Neurosci*. 34: 10430–10437.

Myrick JG. 2015. Emotion regulation, procrastination, and watching cat videos online: who watches internet cats, why, and to what effect? *Comput Hum Behav*. 52:168–176.

Nathoo FS, Masson MEJ. 2016. Bayesian alternatives to null-hypothesis significance testing for repeated-measures designs. *J Math Psychol*. 72:144–157.

Neffati S Taouali O, 2018. An MR brain images classification technique via the Gaussian radial basis kernel and SVM. In *2017 18th International Conference on Sciences and Techniques of Automatic Control and Computer Engineering (STA)* (pp. 611–616). IEEE.

Nelder JA, Wedderburn RWM. 1972. Generalized linear models. *J R Stat Soc*. 135:370–384.

Nenadic I, Güllmar D, Dietzek M, Langbein K, Steinke J, Gaser C. 2015. Brain structure in narcissistic personality disorder: a VBM and DTI pilot study. *Psychiatry Res Neuroimaging*. 231:184–186.

O'Donoghue T, Rabin M. 1999. Incentives for procrastinators. *Discussion Papers*. 114:769–816.

Ochsner KN, Gross JJ. 2005. The cognitive control of emotion. *Trends Cogn Sci*. 9:242–249.

Okuda J, Fujii T, Ohtake H, Tsukiura T, Tanji K, Suzuki K, Kawashima R, Fukuda H, Itoh M, Yamadori A. 2003. Thinking of the future and past: the roles of the frontal pole and the medial temporal lobes. *NeuroImage*. 19:1369–1380.

Ozay M, Esnaola I, Yarman Vural FT, Kulkarni SR, Poor HV. 2017. Machine learning methods for attack detection in the smart grid. *IEEE Trans Neural Netw Learn Sys*. 27:1773–1786.

Özer BU, Demir A, Ferrari JR. 2009. Exploring academic procrastination among Turkish students: possible gender differences in prevalence and reasons. *J Soc Psychol*. 149:241–257.

Panizzon MS, Fennema-Notestine C, Eyler LT, Jernigan TL, Prom-Wormley E, Neale M, Jacobson K, Lyons MJ, Grant MD, Franz CE. 2009. Distinct genetic influences on cortical surface area and cortical thickness. *Cereb Cortex*. 19:2728–2735.

Peters J, Büchel C. 2010. Episodic future thinking reduces reward delay discounting through an enhancement of prefrontal-mediotemporal interactions. *Neuron*. 66:138–148.

Peters J, Büchel C. 2011. The neural mechanisms of inter-temporal decision-making: understanding variability. *Trends Cogn Sci*. 15:227–239.

Petrovic P, Ekman CJ, Klahr J, Tigerström L, Rydén G, Johansson AGM, Sellgren C, Golkar A, Olsson A, Öhman A. 2016. Significant grey matter changes in a region of the orbitofrontal cortex in healthy participants predicts emotional dysregulation. *Soc Cogn Affect Neurosci*. 11:1041.

Phan KL, Fitzgerald DA, Nathan PJ, Moore GJ, Uhde TW, Tancer ME. 2005. Neural substrates for voluntary suppression of negative affect: a functional magnetic resonance imaging study. *Biol Psychiatry*. 57:210.

Pike DJ, Sokal RR, Rohlf PJ. 1981. *The principles and practice of statistics in biological research*. Vol 133. New York (NY): W.H. Freeman, pp. 207–214.

Pine A, Seymour B, Roiser JP, Bossaerts P, Friston KJ, Curran HV, Dolan RJ. 2009. Encoding of marginal utility across time in the human brain. *J Neurosci*. 29:9575.

Piras F, Piras F, Chiapponi C, Girardi P, Caltagirone C, Spalletta G. 2013. Widespread structural brain changes in OCD: a systematic review of voxel-based morphometry studies. *Cortex*. 62:89–108.

Pychyl TA, Lee JM, Thibodeau R, Blunt A. 2000. Five days of emotion: an experience sampling study of undergraduate student procrastination. *J Soc Behav Pers*. 15:239.

Race E, Keane MM, Verfaellie M. 2011. Medial temporal lobe damage causes deficits in episodic memory and episodic future thinking not attributable to deficits in narrative construction. *J Neurosci*. 31:10262–10269.

Rajapakse JC, Giedd JN, Rapoport JL. 1997. Statistical approach to segmentation of single-channel cerebral MR images. *IEEE Trans Med Imaging*. 16:176–186.

Rebetez MML, Barsics C, Rochat L, D'Argembeau A, Van der Linden M. 2016. Procrastination, consideration of future

consequences, and episodic future thinking. *Conscious Cogn*. 42:286–292.

Rebetez MML, Rochat L, Barsics C, Van der Linden M. 2018. Procrastination as a self-regulation failure: the role of impulsivity and intrusive thoughts. *Psychol Rep*. 121:26–41.

Ridgway GR, Omar R, Ourselin S, Hill DL, Warren JD, Fox NC. 2009. Issues with threshold masking in voxel-based morphometry of atrophied brains. *NeuroImage*. 44:99–111.

Román FJ, Lewis LB, Chen CH, Karama S, Burgaleta M, Martínez K, Lepage C, Jaeggi SM, Evans AC, Kremen WS. 2015. Gray matter responsiveness to adaptive working memory training: a surface-based morphometry study. *Brain Struct Funct*. 221:1–14.

Rozental A, Forsell E, Svensson A, Forsström D, Andersson G, Carlbring P. 2014. Psychometric evaluation of the Swedish version of the pure procrastination scale, the irrational procrastination scale, and the susceptibility to temptation scale in a clinical population. *BMC Psychol*. 2:54.

Rozental A, Forsström D, Lindner P, Nilsson S, Mårtensson L, Rizzo A, Andersson G, Carlbring P. 2018. Treating procrastination using cognitive behavior therapy: a pragmatic randomized controlled trial comparing treatment delivered via the internet or in groups. *Behav Ther*. 49:180–197.

Schacter DL, Addis DR, Hassabis D, Martin VC, Spreng RN, Szpunar KK. 2012. The future of memory: remembering, imagining, and the brain. *Neuron*. 76:677–694.

Schacter DL, Benoit RG, Szpunar KK. 2017. Episodic future thinking: mechanisms and functions. *Curr Opin Behav Sci*. 17:41–50.

Schoelkopf B, Sung K, Burges C, Girosi F, Niyogi P, Poggio T, Vapnik V. 2002. Comparing support vector machines with Gaussian kernels to radial basis function classifiers. *IEEE Trans Signal Process*. 45:2758–2765.

Shaw P, Sharp W, Sudre G, Wharton A, Greenstein D, Raznahan A, Evans A, Chakravarty MM, Lerch JP, Rapoport J. 2015. Subcortical and cortical morphological anomalies as an endophenotype in obsessive-compulsive disorder. *Mol Psychiatry*. 20:224–231.

Sirois F, Pychyl T. 2013. Procrastination and the priority of short-term mood regulation: consequences for future self. *Soc Personal Psychol Compass*. 7:115–127.

Sirois FM. 2004. Procrastination and counterfactual thinking: avoiding what might have been. *Br J Soc Psychol*. 43:269–286.

Sirois FM. 2014a. Absorbed in the moment? An investigation of procrastination, absorption and cognitive failures. *Pers Individ Differ*. 71:30–34.

Sirois FM. 2014b. Procrastination and stress: exploring the role of self-compassion. *Self Identity*. 13:128–145.

Smith SM, Nichols TE. 2009. Threshold-free cluster enhancement: addressing problems of smoothing, threshold dependence and localisation in cluster inference. *NeuroImage*. 44:83–98.

Sowell ER, Peterson BS, Kan E, Woods RP, Yoshii J, Bansal R, Xu D, Zhu H, Thompson PM, Toga AW. 2007. Sex differences in cortical thickness mapped in 176 healthy individuals between 7 and 87 years of age. *Cereb Cortex*. 17:1550–1560.

Spielberger CD, Gorsuch RL. 1983. Consulting Psychologists Press, Palo Alto, CA. *Manual for the state-trait anxiety inventory*.

Sporns O, Tononi G, Kötter R. 2005. The human connectome: a structural description of the human brain. *PLoS Comput Biol*. 1:e42.

Sridharan D, Levitin DJ, Menon V. 2008. A critical role for the right fronto-insular cortex in switching between central-executive and default-mode networks. *Proc Natl Acad Sci USA*. 105:12569–12574.

Steel P. 2007. The nature of procrastination: a meta-analytic and theoretical review of quintessential self-regulatory failure. *Psychol Bull*. 133:65.

Steel P. 2010. Arousal, avoidant and decisional procrastinators: do they exist? *Personal Individ Differ*. 48:926–934.

Steel P, Ferrari J. 2013. Sex, education and procrastination: an epidemiological study of Procrastinators' characteristics from a global sample. *Eur J Personal*. 27:51–58.

Steel P, Klingsieck KB. 2016. Academic procrastination: psychological antecedents revisited. *Aust Psychol*. 51:36–46.

Studholme C, Cardenas V, Maudsley A, Weiner M. 2003. An intensity consistent filtering approach to the analysis of deformation tensor derived maps of brain shape. *NeuroImage*. 19:1638–1649.

Studholme C, Cardenas V, Schuff N, Rosen H, Miller B. 2001a. In: Weiner M, editor. Detecting spatially consistent structural differences in Alzheimer's and fronto temporal dementia using deformation morphometry. In *International Conference on Medical Image Computing and Computer-Assisted Intervention* (pp. 41–48). Springer, Berlin, Heidelberg.

Studholme C, Novotny E, Zubal IG, Duncan JS. 2001b. Estimating tissue deformation between functional images induced by intracranial electrode implantation using anatomical MRI. *NeuroImage*. 13:561–576.

Su T, Guo Y Q, Chen Z Y, et al. (2019). The neural basis underlying procrastination: a large-scale study of brain networks (in Chinese). *Sci Sin Vitae*. 49:77–88, doi: 10.1360/N052018-00158.

Svartdal F. 2017. Measuring procrastination: psychometric properties of the Norwegian versions of the irrational procrastination scale (IPS) and the pure procrastination scale (PPS). *Scand J Educ Res*. 61:18–30.

Svartdal F, Steel P. 2017. Irrational delay revisited: examining five procrastination scales in a global sample. *Front Psychol*. 8: 1927.

Talairach J, Tournoux P, Rayport TBM, Tournoux P. 1988. *Co-planar stereotaxic atlas of the human brain: 3-dimensional proportional system: an approach to cerebral imaging*. Thieme Medical Publishers, New York.

Tibshirani R. 1996. Regression shrinkage and selection via the LASSO. *J R Stat Soc B Methodol*. 58:267–288.

Tibshirani R. 2011. Regression shrinkage and selection via the LASSO: a retrospective. *J R Stat Soc B Statist Methodol*. 73:273–282.

Tice DM, Bratslavsky E. 2000. Giving in to feel good: the place of emotion regulation in the context of general self-control. *Psychol Inq*. 11:149–159.

Tice DM, Bratslavsky E, Baumeister RF. 2001. Emotional distress regulation takes precedence over impulse control: if you feel bad, do it! *J Pers Soc Psychol*. 80:53.

Tohka J, Zijdenbos A, Evans A. 2004. Fast and robust parameter estimation for statistical partial volume models in brain MRI. *NeuroImage*. 23:84–97.

Trawiński B, Smętek M, Telec Z, Lasota T. 2012. Nonparametric statistical analysis for multiple comparison of machine learning regression algorithms. *Int J Appl Math Comput Sci*. 22:449–471.

Uddin LQ. 2015. Salience processing and insular cortical function and dysfunction. *Nat Rev Neurosci*. 16:55–61.

van't Veer AE, Giner-Sorolla R. 2016. Pre-registration in social psychology—a discussion and suggested template. *J Exp Soc Psychol*. 67:2–12.

Van Eerde W. 2000. Procrastination: self-regulation in initiating aversive goals. *Appl Psychol*. 49:372–389.

Vapnik VN. 2002. The nature of statistical learning theory. *Technometrics*. 8:1564–1564.

Wagenmakers E-J, Love J, Marsman M, Jamil T, Ly A, Verhagen J, Selker R, Gronau QF, Dropmann D, Boutin B. 2018. Bayesian inference for psychology. Part II: Example applications with JASP. *Psychonomic Bull Rev*. 25:58–76.

Wasserstein RL, Lazar NA. 2016. The ASAs statement on p-values: context, process, and purpose. *Am Stat*. 70:129–133.

Whelan R, Conrod PJ, Poline J-B, Lourdusamy A, Banaschewski T, Barker GJ, Bellgrove MA, Büchel C, Byrne M, Cummins TD. 2012. Adolescent impulsivity phenotypes characterized by distinct brain networks. *Nat Neurosci*. 15:920.

Wu Y, Li L, Yuan B, Tian X. 2016. Individual differences in resting-state functional connectivity predict procrastination. *Pers Individ Differ*. 95:62–67.

Yang C, Wu S, Lu W, Bai Y, Gao H. 2014. Anatomic differences in early blindness: a deformation-based morphometry MRI study. *J Neuroimaging*. 24:68–73.

Yotter RA, Dahnke R, Gaser C. 2011a. Topological correction of brain surface meshes using spherical harmonics. *Hum Brain Mapp*. 32:1109–1124.

Yotter RA, Nenadic I, Ziegler G, Thompson PM, Gaser C. 2011b. Local cortical surface complexity maps from spherical harmonic reconstructions. *NeuroImage*. 56: 961–973.

Zhang S, Becker B, Chen Q, Feng T. 2019a. Insufficient task-outcome association promotes task procrastination through a decrease of hippocampal-striatal interaction. *Hum Brain Mapp*. 40:597–607.

Zhang S, Feng T. 2019. Modeling Procrastination: Asymmetric Decisions to Act Between the Present and the Future. Journal of Experimental Psychology: General. Advance online publication. 10.1037/xge0000643.

Zhang S, Liu P, Feng T. 2019b. To do it now or later: the cognitive mechanisms and neural substrates underlying procrastination. *Wiley Interdiscip Rev Cogn Sci*. 10:e1492.

Zhang W, Wang X, Feng T. 2016. Identifying the neural substrates of procrastination: a resting-state fMRI study. *Sci Rep*. 6:33203.

Zhang Z, Ling HE, Shi Z. 2017. A randomized controlled trial of solution-focused brief group counseling on procrastination in graduate students. *Chin Ment Health J*. 31:7–12.

Ziesat HA Jr, Rosenthal TL, White GM. 1978. Behavioral self-control in treating procrastination of studying. *Psychol Rep*. 42:59–69.